EXPERIMENTAL INVESTGATION ON PREMIXED OXY-COMBUSTION AT CONSTANT REYNOLDS NUMBERS

BY

Shabeeb Ali Alkhaldi

A Thesis Presented to the
DEANSHIP OF GRADUATE STUDIES

KING FAHD UNIVERSITY OF PETROLEUM & MINERALS

DHAHRAN, SAUDI ARABIA

In Partial Fulfillment of the
Requirements for the Degree of

MASTER OF SCIENCE

In

MECHANICAL ENGINEERING

April 2018

KING FAHD UNIVERSITY OF PETROLEUM & MINERALS

DHAHRAN- 31261, SAUDI ARABIA

DEANSHIP OF GRADUATE STUDIES

This thesis, written by **SHABEEB ALI ALKHALDI** under the direction of his thesis advisor and approved by his thesis committee, has been presented and accepted by the Dean of Graduate Studies, in partial fulfillment of the requirements for the degree of **MASTER OF SCIENCE IN MECHANICAL ENGINEERING.**

Dr. Mohamed A. Habib
(Advisor)

Dr. Zuhair Gasem
Department Chairman

May-8
2018

Dr. Medhat A. Nemitallah
(Member)

Dr. Salam A. Zummo
Dean of Graduate Studies

Dr. Syed A. Said
(Member)

15/5/19

Date

Dedicated to my loved father and mother whose presence, and prayers are the reason for the success in my life.

Acknowledgment

All compliments go to Almighty Allah for giving me courage and stability to succeed in this work. I would love to express my great thanks and gratitude to Almighty Allah for providing me the opportunity to do my M.S. at King Fahd University of Petroleum and Minerals. I am very glad to have had an opportunity to praise His name in the sincerest way through this accomplishment and ask him to accept my efforts.

My deep gratitude and appreciation goes to my thesis advisor professor M. Habib for his constant guidance, motivation and support during my studies. His valuable and priceless suggestions and ideas made this work interesting and challenging for me. I also want to express my deep appreciation to Dr. M. Nemitallah and Dr. A. Abdelhafez for their help, guidance, and constant encouragement during my M.S. Special thanks go to Professor S. Said for his help and support.

Great thanks also go to my friends Mr. B. Imtiyaz, Mr. M. Aliyu and Mr. S. Rashwan who helped and assisted me during my study.

TABLE OF CONTENTS

LIST OF TABLES

LIST OF FIGURES

LIST OF ABBREVIATIONS

CH_4	:	Methane
CO_2	:	Carbon dioxide
D	:	Throat diameter (2 cm)
D_{in}	:	Inlet diameter (cm)
f	:	Azimuthal spinning frequency
IRZ	:	Inner recirculation zone
ISL	:	Inner shear layer
mt	:	Million tons
$\dot{m}$	:	Mass flow rate (kg/s)
mps	:	Meter per second
O_2	:	Oxygen
OF	:	Oxygen Fraction
ORZ	:	Outer recirculation zone
PD	:	Power density ($MW/m^3/bar$)
Re	:	Reynold number
St	:	Strouhal number
Sw	:	Swirl number

T_{ad}	:	Adiabatic flame temperature (K)
U_{in}	:	Inlet velocity (m/s)

Greek Symbols

φ	:	Equivalence ratio
ρ	:	Flow density (kg/m^3)
μ	:	Dynamic viscosity (Pa.s)

Abstract

Full Name : Shabeeb Ali Ebdah Alkhaldi

Thesis Title : Experimental Investigation On Premixed Oxy-Combustion At Constant Reynolds Numbers

Major Field : Mechanical Engineering

Date of Degree : April 2018

In this study, the static stability limits, in terms of blow-out and flash back, and the changes in macrostructure of fully premixed oxy-methane flames in a swirl combustor were recorded experimentally. The data under fixed Reynolds number (*Re*) operation were recorded to isolate its dynamic effect on flame stabilization and understand clearly the physics behind the oxy-flame extinction mechanisms. Three sets of experiments were conducted, each at a fixed *Re*, namely 7000, 9000 and 11000. At a given *Re* operation, the limits are recorded under fixed inlet bulk flow velocity (U_{in}) while varying the oxygen mole fraction (*OF*: from 29% to 70%) and the equivalence ratio (φ: from 0.2 to 1.0). Two-dimensional (2-D) stability maps are presented at fixed *Re*operation as function of φ and *OF*. The maps are presented on the contours of inlet velocity (U_{in}), combustor power density (*PD*) and adiabatic flame temperature (T_{ad}) to correlate these parameters with flame static stability limits. Selected flames were imaged to record the different flame stabilization modes and changes in flame macrostructure toward the limits and to analyze the effects of equivalence ratio (φ), oxygen fraction (*OF*), inlet velocity (U_{in}), adiabatic flame temperature (T_{ad}) and Reynold number (*Re*) on flame stability. Temperature measurements are provided to quantify the effects of *OF* and *Re* on local flame temperature, and to serve as data base for validating the numerical models. It is observed that it is not possible to sustain premixed oxy-methane flames in the *OF* ranges

below 29% and above 70%. The results show that the reactions kinetic rate is a more relevant parameter than *Re* for determining the flame speed and, consequently, the flashback limit. Under all operating *Re* values, the flames blow-out at the same power density (*PD*) of 3.0 MW/m^3/bar. This indicates the leading role of *PD* for controlling flame stability near the lean blow-out limit. Increasing *Re* widens the operability range of the flame by shifting the blow-out limit toward leaner conditions. The analysis of the changes in flame macrostructure shows that U_{in} is a more relevant parameter than *Re* for controlling the equivalence ratio at which flame transition from the inner shear layer (ISL) to the outer recirculation zone (ORZ) occurs. Increasing U_{in} retards the flame transition towards leaner operation and closer to the lean blow-low out limit. Similar flame macrostructures can be obtained while fixing one flow characteristic parameter (*Re*) and one flame characteristic parameter (T_{ad}). Oxygen fraction has a major controlling role on the flame macrostructure and stability. Flames do not hold fixed macrostructure neither near flashback nor near blow-out limits. The flames at lower *Re* blow-out without being lifted. At higher *Re*, the flames encounter stabilization in the ORZ followed by lift-off before being blown-out.

ملخص الرسالة

الاسم الكامل: شبيب علي ابداح الخالدي

عنوان الرسالة: التحقيق العملي على غاز الأكسجين مسبق الخلط في المفاعل عند أرقام رينولدز ثابتة.

التخصص: هندسة ميكانيكية

تاريخ الدرجة العلمية: أبريل ٢٠١٨ م

في هذه الدراسة، تم عمليا تسجيل حدود الإستقرار الثابتة عن طريق معرفة انطفاء واسترجاع اللهب، وكذلك تغيرات الشكل العام للهب الناتج عن استخدام غازات الأكسجين والميثان مسبقة الخلط في دوامة المفاعل. تم تسجيل النتائج عند رقم رينولدز ثابت من أجل عزل تأثيره الديناميكي على إستقرار اللهب ، و كذلك من أجل فهم الفيزياء من وراء آلية انقراض لهب الأكسجين. تم إنجاز ثلاث تجارب عملية كل واحدة منها عند رقم رينولدز معين تحديدا ٧٠٠٠، ٩٠٠٠، ١١٠٠٠. عند كل رقم رينولدز تم تسجيل حدود إستقرار اللهب باستخدام سرعة ثابتة مع تغيير نسبة الأكسجين من ٢٩% إلى ٧٠% ، وكذلك تغيير نسبة التكافؤ من ٠,٢ إلى ١. خرائط حدود الإستقرار ثنائية الأبعاد تم عرضها عند رقم رينولدز ثابت مع تغيير نسبة الأكسجين و نسبة التكافؤ. الخرائط عرضت على خلفية محيط شكل السرعة، وكثافة الطاقة، وأيضا درجة حرارة اللهب القصوى من أجل ربط هذه العوامل مع حدود إستقرار اللهب.

تم أخذ صور لأشكال لهب معينة ، من أجل تسجيل الإختلافات في مواضع إستقرار اللهب ، وكذلك التغيرات في الشكل العام للهب ، و أيضا تحليل تأثير نسبة التكافؤ ، نسبة الأكسجين ، سرعة الإدخال ، و درجة حرارة اللهب القصوى على استقرار اللهب. تم عرض قياس درجات الحرارة في هذه الدراسة من أجل تحديد تأثير نسبة الأكسجين و رقم الرينولدز على حرارة اللهب المحلية ، و كذلك توفير قاعدة بيانات للتحقق من صحة النماذج الرقمية.

لوحظ من خلال التجارب العملية أنه لا يمكن الحفاظ على لهب الأكسجين مع الميثان مسبق الخلط عنما تكون نسبة الأكسجين المستخدمة أقل من ٢٩% و أكثر من ٧٠%. أظهرت النتائج أن عامل معدل التفاعل الحركي أكثر أهمية من عامل رقم الرينولدز في في تحديد سرعة اللهب ، و في ظاهرة إسترجاع اللهب. في كل أرقام الرينولدز المستخدمة ينطفئ اللهب عند كثافة طاقة متساوية ٣ م و/ م^{٣} / بار ، مما يدل على الدور القيادي لعامل كثافة الطاقة في التحكم في إستقرار اللهب عندما يكون بالقرب من حد الإنطفاء. أثبتت الدراسة أن زيادة رقم الرينولدز يوسع عمليات تشغيل اللهب من خلال نقل حد إنطفاء اللهب إلى ظروف الحرق الضعيف (زيادة نسبة الهواء الزائد عن الإحتراق).

أظهرت التحاليل في تغيرات الشكل العام للهب أن عامل سرعة الإدخال أكثر أهمية من عامل رقم الرينولدز في عملية التحكم في نسبة التكافؤ عند تحول اللهب من طبقة القص الداخلية إلى منطقة التدوير الخارجية. أشارت النتائج إلى أن إرتفاع سرعة الإدخال يؤخر إنتقال اللهب نحو ظروف الحرق الضعيف و القرب من حدود الإنطفاء.

شكل لهب متطابق ممكن الحصول عليه عند تثبيت عامل من خصائص التدفق (رقم رينولدز) ، و عامل من خصائص اللهب (درجة الحرارة القصوى). لوحظ من خلال الدراسة أن نسبة الأكسجين لها تأثير كبير في التحكم في تركيبة اللهب و استقراره ، كذلك أظهرت النتائج أن اللهب لا يحمل تركيبة واحدة سواء بالقرب من حد إرتجاع اللهب أو إنطفائه. عند رقم رينولدز منخفض ، اللهب ينطفئ من دون أن يرتفع ، بينما عند رقم رينولدز أعلى ، اللهب يستقر في منطقة التدوير الخارجية ثم يرتفع إلى الأعلى ثم ينطفئ.

CHAPTER 1

INTRODUCTION

1.1 Combustion technologies

The combustion of fossil fuels is the main procedure for producing power. Due to its hazardous effects on the environment in terms of NO_x, SO_x, and carbon emissions [1], with the latter being the main cause of the greenhouse effect and hence increase the fear of global warming, many technologies have been invented to reduce those effects [2]. Carbon Capture and Storage (CCS) technology is an effect way to decrease the dangerous of these pollutants [3]. There are three methods in Carbon Capture Technology: pre-combustion, oxy-combustion, and post-combustion [4]. In post-combustionmethod, filters are used to capture CO_2 after the combustion process. While in pre-combustion method, gasification is used to remove the carbon component before the combustion process. In oxy-combustion process, pure oxygen is used to burn the fuel, which results in combustion products consisting of CO_2 and H_2O. In this process, CO_2 is captured after condensing the products. Oxy-fuel combustion process is illustrated in figure 1. Oxy-fuel combustion is preferred method for capturing the CO_2 emissions, because it has an easy application in industrial furnaces [5-8]. Also, it contains more oxygen concentration which makes its adiabatic flame temperature more than the adiabatic flame temperature of a hydrocarbon fuel and air flame [9]. As a result of the higher temperature of the oxy-fuel flame, its distinguished by a faster chemical reaction. Moreover, the oxy-combustion

technology is preferred because the volume and mass of the flue gas are reduced and hence the size of the flue gas equipment treatment decreased. Due to this decrease, the CO_2 concentration increase making the concentration easy to separate [10]. Additional benefits of oxy-combustion are eliminating the NO_x emissions because the N_2 gas is eliminated from the reactants [11]. Nowadays, lean premixed combustion is the most applied technology in gas turbines due to its high efficiency and low emission power generation. Lean premixed combustion technique is very effective and favorable because it produces power at low NO_x emissions due to lowered combustion temperature within the combustor [12]. From the discussion above we can say that lean premixed oxy-combustion would keep the environment safe from pollutants.

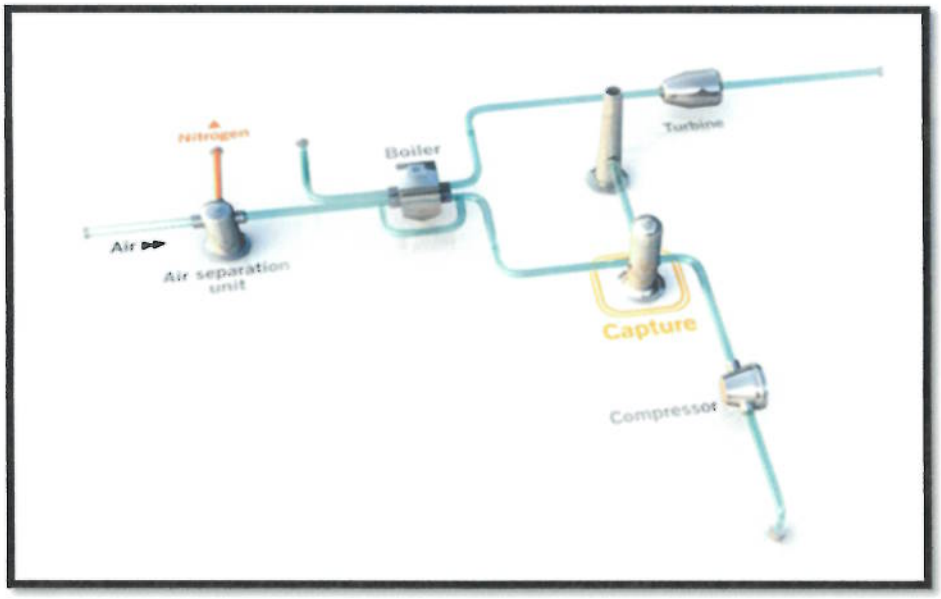

Figure 1 Oxy-fuel combustion process [13].

1.2 Problem Statement

The use of gas turbines in combined cycle power plants is an effective and important technology for power generation, especially in Saudi Arabia. According to table 1 Saudi

Arabia produce 604.27 billion kWh from fossil fuel. This large use of fossil fuel causes a serious damage to the environment. One of the dangerous effects of the fossil fuel is the high production of CO_2 emissions. Figure 2 illustrates the increase of CO_2 emissions in Saudi Arabia from 1992 to 2014. The CO_2 production has increased from 295 mt to 600 mt in 2014 which make the government to put strict regulations of harmful pollutants emissions, keeping much pressure on the development and adaptation of gas turbines to match such regulations. The present study will focus on the analysis of premixed oxy-fuel combustion in a gas turbine combustor experimentally. The goal of this study is to help to solve problems affecting the environment such as emissions of pollutant that cause global warming. Also, this study should help in solving problems associated with emission control, temperature distribution and flame stability in gas turbine combustors. The experimental setup is based on the existing setup available in the clean combustion Laboratory at King Fahd University of Petroleum and Minerals.

Table 1 Energy sources and consumptions in Saudi Arabia and Europe [14].

Energy source	Total in Saudi Arabia	percentage in Saudi Arabia	percentage in Europe	per capita in Saudi Arabia	per capita in Europe
Fossil fuels	604.27 bn kWh	99,9 %	48,9 %	18,722.24 kWh	7,993.04 kWh
Nuclear power	0.00 kWh	0,0 %	7,2 %	0.00 kWh	1,185.60 kWh
Water power	0.00 kWh	0,0 %	23,4 %	0.00 kWh	3,829.04 kWh
Renewable energy	604.88 m kWh	0,1 %	16,2 %	18.74 kWh	2,654.74 kWh
Other energy sources	0.00 kWh	0,0 %	4,3 %	0.00 kWh	696.01 kWh
Total production capacity	604.88 bn kWh	100,0 %	100,0 %	18,740.98 kWh	16,358.42 kWh

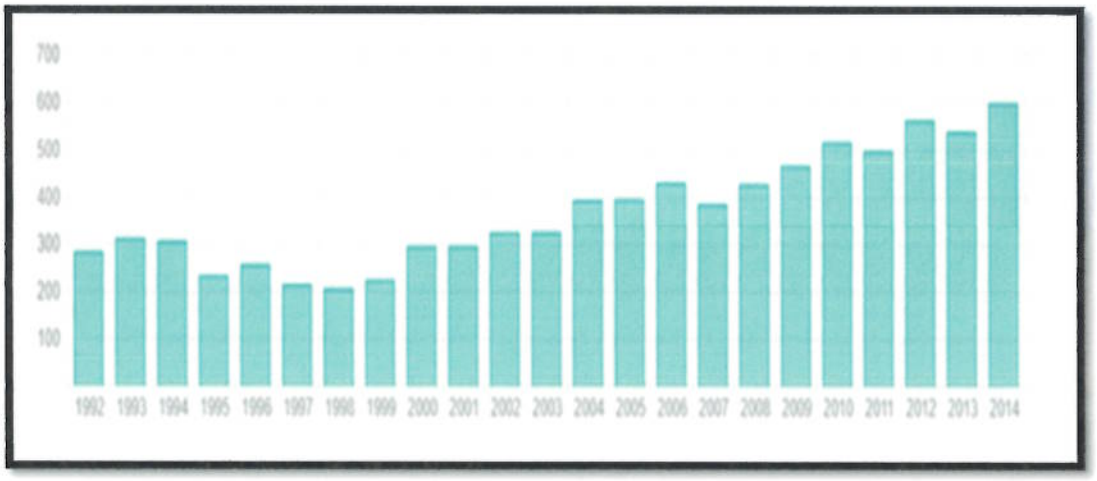

Figure 2 Development of CO_2 emissions in million tons in Saudi Arabia from 1991 to 2014 [14].

1.3 Objectives

The main objective of this research is to study experimentally the effect of different operating parameters on the characteristics of premixed oxy-fuel combustion in a gas turbine combustor. The specific objectives are:

- To study experimentally the lower and upper flammability limits, visual appearance and the extinction mechanisms of premixed oxy-combustion flames at fixed inlet Reynolds and fixed inlet velocity using different equivalence ratio and oxygen fraction in a gas turbine combustor.
- To study the effect of Reynolds number, inlet velocity, oxygen fraction, equivalence ratio, Adiabatic flame temperature, and power density on combustion instabilities and flame macrostructure.
- To provide a benchmark experimental data of premixed oxy-combustion of methane at different operating conditions including oxidizer composition and fuel volume flow rate.

CHAPTER 2

LITERATURE REVIEW

This literature review focuses on the experimental and numerical studies completed in the area of oxy-combustion in gas turbines.

2.1 Premixed Oxy-combustion

Using CO_2 as a diluent instead of N_2 effects the combustion process due to the differences in the radiative release, chemical kinetic and thermo-physical properties [15-19]. Utilizing CO_2 provide more radiative heat exchange with the surrounding compared with air flames [20]. Many studies have discussed premixed oxy-combustion in a swirl stabilized system [17, 19, 21, and 22]. Lean premixed combustion is achieved when the oxidizer and the fuel are mixed prior reaching to the combustor at an equivalence ratio less than one. Lean premixed combustion is used in almost all combustion technology areas such as gas turbines, and furnaces [23]. This technology provides less emission and more efficiency. Emissions are low because the flame temperatures are reduced which reduces the thermal nitric oxide formation [24]. Also, CO emissions decrease due to high efficiency. Oxy-fuel combustion is an effective technology for reducing the CO_2 emissions up to 20% by capturing and sequestration. It utilizes oxygen instead of air and hence eliminates nitrogen from the oxidant gas stream [25]. Kim et al. [26] studied the flame features of H_2 enriched methane-air premixed swirling flames operating below fuel lean combustion conditions. A swirl stabilized laboratory scale of 5.82 kW premixed

combustor was made to study the impact of H_2 increment and swirl on the combustion of premixed flames. A particle image velocimetry was utilized for studying the effect of H_2 enriched methane flames on flow field. The results presented that, at the top region of the reaction zone the flame area increased and this was related to the higher availability of ignition from the recirculation flow. Seiser et al. [27] analyzed the characteristics of laminar partially premixed flames specifically the flammability limit and the extinction using counter flow configuration on a wide domain of partial premixing. The results showed that flame temperature decreases while increasing the level of premixing. The impact of CO_2 dilution on the laminar flame speed of premixed methane-air combustion stable on a flat burner were experimentally studied by Chan et al. [28] the results indicated that as the CO_2 percentage increases in the mixture the laminar flame speed of the air-methane combustion reduces. Li et al. [29] analyzed the impact of the flue gas recirculation on the premixed flames at atmospheric condition. They showed that as the concentration of N_2, H_2O and CO_2 into O_2/CH_4 flame increases, the flame temperature and the burning velocity decreases. Watanabe et al. [30] made a comparison between lean air-flames and lean oxy-flames in a premixed swirl combustor. The result showed differences in the flame shape when comparing oxy-flames and air-flames especially when the equivalence ratio reaches 0.60 at the same Reynolds number, swirl number, adiabatic temperature, and equivalence ratio. Griebel et al. [31] experimentally studied the lean blowout limits and NO_x emissions of lean premixed, hydrogen enriched methane/air flames at high pressure. The operating parameters were pressure of 14 bar, bulk velocity range from 32 to 80 m/s and two preheating temperature 673 K, 773 K. The results show that due to the extinction of the Lean Blowout limits for hydrogen addition,

lower minimum NO_x can be observed due to lower flame temperature at lower equivalence ratio. Jamal et al. [32] experimentally studied the structure and lean extinction of premixed liquefied petroleum gas-air flames on a perforated plate. It is found that thicker plates provide a slightly better stability characteristic and that attributed to greater amount of heat transfer inside them.

2.2 Flame Instabilities

Combustion noise, blow-off and lift-off recognize the flame instability [33]. Combustion instability is an oscillatory fluid motion which occurs because of coupling unsteady fluid mechanics and the combustion process [34-36]. Combustion instabilities occur when a positive feedback is achieved between the heat release and the acoustic environment [37]. There are different parameters that affect the combustion stability such as combustor geometry and the associated flame anchoring mechanism. The combustor geometry effects the construction of the recirculation zone build to stabilize the flame [38]. Speth and Ghoniem [39] studied the combustion instabilities over different operating conditions. The results showed that combustor geometry strongly affect the combustion instabilities. Kutne et al. [40] completed a study on the partially premixed swirl stabilized oxy-fuel combustion performed at atmospheric pressure using in a gas turbine combustor. The results indicated that the oxygen has a major impact on the combustion in opposite to the equivalence ratio that has less effect. They observed that as the oxygen fraction increase, the stable flames are noticed at much leaner condition. Rashwan et al. [41] experimentally analyzed the impact of partial premixed on oxy-combustion. They showed that oxygen concentration from 29% to 40% provide a stable flame condition.

They also showed that oxy-combustion has smaller stability values than the air combustion which is attributed to the impact of involving CO_2 in the process. Rashwan et al. [42] experimentally analyzed the partially premixed oxy-combustion flames on a perforated plate burner at atmospheric conditions. They showed that while raising the oxidizer Reynolds number, the flammability limit increase, caused by increasing the momentum and mixing levels. They also stated that it is not possible to operate below an oxygen fraction of 29%. The stable flame operation noticed at oxygen fraction 36%. Kimura et al. [43] proposed that more oxygen fraction and more gas temperature in the flue gas would relive the combustion instability. Also, higher steam ratio in the flue gas would raise the efficiency of the oxy-fuel combustion.

Fujimori and Yamada [44] completed projects for understanding the oxy-fuel combustion power plant for carbon storage. They showed that the velocity of the flame in the O_2/CO_2 mixture decreased compared with the air mixture. Also, they observed that the O_2 concentration must increase to have a stable flame in oxy-combustion mode. Zhang et al. [45] concluded that flame stabilization can be approached at low equivalence ratios and low adiabatic flame temperatures at laminar flame speed with an increase in H_2 percentage. Riahi et al. [46] studied the impact of mixed oxygen and hydrogen below lean conditions. The study showed that enrichment of oxygen and hydrogen makes the operations under low ranges of richness and has more stable flame. Nemitallah et al. [47] experimentally and numerically discussed diffusion oxy-flames in different combustors.

They stated that when operating at an equivalence ratio less than 25% the stability of the combustion flames is affected.

2.3 Blow-off

Blow-off phenomena occur when the flame is separated from the combustion base and basically blown-off the combustor which causes the flame extinction. This phenomenon is observed from flame images [48]. Blow-off limits are essential in operation of gas turbine which is affected by many factors such as geometric swirl number, and combustion process [49]. Daniele et al. [50] studied the lean premixed syngas combustion considering the blow out limits, turbulent flame speed and emissions. A high-pressure combustor is utilized in the experiment. The results indicate that when H_2 increases in the fuel mixture at which Lean Blowout flame occurs, the equivalence ratio become leaner. It is found that the adiabatic flame temperature has a major effect on the NO_x emissions of all experimented fuel mixture. Cavaliere et al. [51] experimentally studied premixed methane with air in a combustion chamber by an axial annular swirl generator. The results showed that at swirl number equal to 1.25 a loss of flame stability and blow-off occurred when the equivalence ratio reduced to 0.57. Amato et al. [52] studied the lean blow-off limit. They showed that the operation boundaries of the CO_2 diluted system decrease more than methane-air mixture in a premixed swirl combustor which caused by

the slower kinetics of $CH_4/O_2/CO_2$. At an adiabatic temperature of 300k the CO_2 diluted mixture blow-off which is higher than that of air mixture. Hoffman et al. [53] related the Blow-off phenomena of the combustion to the very lean mixture, high combustion Instabilities and short hold-up time of reagents as compared to the time corresponding to characteristics time for chemical reaction according to the Damkholer number ($Da = \tau_{res}/\tau_{chem}$). A small Damkholer number less than one indicate a small chemical reaction while a Damkholer number greater than one indicates high chemical reaction. When Damkholer number is low, flame extinction and blow-out occur which means when the ratio of flow mixing time to the chemical reaction time is not high enough [54-56]. Abdulsada [57] studied the limits of flame blow-off in an open space. He used a conical metal burner caps and swirl generator with a tangential supply of combustible mixtures. Burner caps are used to prevent cold air from entering to the flame and hence improve the Blow-off limits. The results showed that conical fitting is better for flame Blow-off regardless of the swirl number 0.8 and 1.04 and the fuel used in the experiment.

2.4 Numerical Investigations

Many numerical investigations were completed in the area of premixed oxy-combustion and gas turbine combustor and they are presented as follows.

Krieger et al. [58] numerically discussed the characteristics of oxy-combustion utilizing a model of gas turbine combustor. The results presented that the propane/oxy-fuel looks

like the standard situation in propane/air flame, but it has a more temperature in the middle region of the combustor. Xuan and Blanquart [59] numerically studied the effect of two-dimensional flow on soot formation in laminar premixed flames. The results presented that the two-dimensional impacts are essential for all flames studied. Seepana and Jayanti [60] numerically studied the oxy-fuel combustion flame structure. The results indicated that the impact of oxidant dilution on the flame extinction makes the limiting concentration of O_2 in oxy-methane flame equal to 24.5 % by volume, the remaining is CO_2. Schefer et al. [61] studied the features of a premixed swirl-stabilized flame experimentally and numerically. The purpose of the studies is to analyze the impacts of methane added with hydrogen at fuel lean conditions. The study showed that the CO concentration reduced when adding hydrogen. Direct numerical simulation by Hawkes and Chen [62] studied the impact of hydrogen addition in lean premixed methane-air flames. The simulation was performed in which two flames with various fuel mixtures were divided into two similar dimensional flow field. The results showed that higher flame speed received for the enriched flame, which is related to the increased flame speed, higher burning rate, and larger flame surface area. The CO emissions were examined, and the results showed lower CO emissions per methane consumptions for the enriched flame. More CO emissions produced around the flame tolerate downstream interaction, where the volume of CO oxidants is decreased. Erjiang et al. [63] studied numerically and experimentally the investigation of lean methane-hydrogen-air flames at an equivalence ratio equal to 0.8. The results showed that as the initial temperature and hydrogen fraction increase the laminar burning velocity increase. De La Torre et al. [64] studied the impact of hydrogen addition and firing input on premixed oxy-syngas flames.

The results showed that the radiative heat release factor reduces as the firing input increases and hence higher hydrogen concentration will be received. The increase in the radiative heat release will be observed at high equivalence ratio and high recirculation value of diluents of CO_2. The effect of exhaust gas recirculation at atmospheric pressure on premixed oxy-methane flames was numerically studied by Li et al. [65] they concluded that there are changes in the species concentration and change in the flame location for the oxy-methane combustion. Jithin et al. [66] numerically studied the stability of perforated plate stabilized Propane-Air premixed flames using 3-D simulation. The results indicate that as the inlet velocity increases the flame stand-off distance increase. When the equivalence ratio increases, the heat flux to the plate increase where the flame moves toward the plate. Aladawy et al. [67] numerically studied the effect of turbulence on NO_x emissions in a lean premixed combustor running on methane / air at an inlet temperature of 495 K and pressure of 5 atm at equivalence ratios from 0.54 to 0.85. The results show that as the temperature increase in the flame region, the NO_x emission increase with respect to the decrease of turbulence mixing time scale. At fixed turbulent mixing time, the flame zone residence time increase which causes the NO_x emission to increase. The NO_x emission in flame zone is affected by the flame zone residence time when the turbulent mixing time is small. They concluded that as the turbulent mixing time decrease the flame length and flame residence time decrease.

2.5 Adiabatic Flame Temperature

The adiabatic flame temperature is the ultimate temperature occurs during a combustion process for the combustion products when there is no heat loss to the surrounding from

the system is attained [68]. The adiabatic flame temperature is referred to the products for a combustion process that performed in an adiabatically with no shaft work. For a certain oxidizer and fuel, the maximum adiabatic flame temperature observed with a stoichiometric mixture. Many papers have considered the adiabatic flame temperature in the study. Also, several studies show that NO_x emissions level increase with the flame temperature and flow residence time in combustor [69-71].

Buhre et al. [72] concluded that to have an adiabatic flame temperature identical to the one observed in air combustion we must have an oxygen concentration up to 30 %. Kumagami et al. [73] studied the laminar premixed $CH_4/O_2/H_2O$ flames in fuel rich conditions under pressure up to 3 MPa. They found two different Super Adiabatic Flame Temperature (SAFT) regimes. The first one was indicated by equivalence ratio from 1 to 2 and fewer water dilutions. The SAFT phenomena occur less in the first regime with high pressure and occur in the second regime at different pressure conditions. It was also stated that as the pressure increased, the laminar burning velocity decreased in the first regime. Ditranto and Hals [74] studied CO_2/O_2 premixed flames; they concluded that increasing the oxygen volumetric concentration to 30% will provide an adiabatic flame temperature identical to the one obtained in the air-fuel combustion. Liu and Gulder [75] investigated the reaction flux in premixed flames of CH_4/O_2 and CH_4/Air by changing the diffusion properties of H_2 and H radicals. They reported that the Super Adiabatic Flame Temperature (SAFT) phenomena are not caused by the shortage of H-radicals at the end of heat release reactions, neither the preferential of H_2. Stezlner et al. [76] numerically studied the super adiabatic flame temperature in premixed methane flames. The results showed that for equivalence ratio greater than 0.9 the maximum flame temperature

exceeds the equilibrium temperature. Also, pressure decrease causes to reduce the super adiabatic flame temperature for an equivalence ratio from 1 to 2 and to increase it for an equivalence ratio greater than 2.

2.6 Flashback Phenomena

Flashback Phenomena in a lean premixed combustion occurs when the flame propagates into the premixing zone opposite to the flow of the gas stream. Flashback is dangerous because, it increases pollutant emissions, and it can cause damage to the hardware of the premixing zone [77]. Many researchers [78-80] discussed different flashback modes in a swirl stabilized lean premixed turbine combustor. They attributed the flashback occurrence to one of the following reasons: - flame diffusion inside the boundary layer, turbulent flame diffusion in the core flow, violent combustion instabilities and combustion induced vortex breakdown. For the boundary layer flashback case, the flame propagates upstream when it's burning velocity become higher than the local flow velocity. Normally this type of flashback occurs closed to the wall where no slip boundary condition occurs. Turbulent flame propagation in the core flow exists in high swirling flow when the local burning velocity displaces local flow velocity. Swirling flow with swirl number greater than 0.7 stretches the flame surface and excites the start of flashback along the burner axis [81]. Large amplitude pressure fluctuation of acoustic nature [82] that occurs next to stoichiometric operation in a high power, lean flammability, and low emissions combustors, causes instability in the combustion chamber [83]. Sattelmayer et al. [84-85] have showed that Combustion Induced Vortex Breakdown as the general flashback mechanism in swirl stabilized gas turbine combustor.

Vortex breaks down results due to an increase in azimuthal velocity in relation to axial velocity which cause a low flow region in front to it. The vortex breaks down go upstream due to the propagation of the flame upstream. Due to the flame propagation, upstream the flashback occurs even if the burning velocity is less than the flow velocity [86]. Schonborn et al. [87] conducted a study on hydrogen combustion. They attributed the flame flow back to the burner as a result to the occurrence of a strong reverse flow of hot gases in the central recirculation zone. Durox et al. [88] found that thermos-acoustic oscillation is one of the reasons that cause the flame to flashback. Harris et al. [89] attributed the reason of flashback to the propagation of the flame inside the boundary layer relying on a critical velocity gradient. Zhiguang et al. [90] concluded that flame flashback occurs as the turbulent combustor velocity becomes higher than the local velocity of the combustible mixture. They concluded that flashback phenomena occur for systems where the fuel is premixed with the oxidizer. Shelil [91] completed an experimental and numerical studies on methane combustion in an open space for swirl generators with S = 1.47 and 1.54. It is found that 30% addition of CO_2 to CH_4 improved the combustion stability in terms of equivalence ratios in a range of $0.6 < \Phi < 1.2$. Bereer et al. [92] showed an increased tendency of flashback along with increased in pressure and adiabatic flame temperatures of flames.

2.7 Equivalence Ratio & Oxygen Fraction

Equivalence ratio is expressed as the ratio of the stoichiometric oxidizer to fuel ratio to the actual oxidizer to fuel ratio. Shi et al. [93] experimentally studied the impact of carbon dioxide dilution in oxygen-methane combustion. The results showed that stable

flame is found for a range of equivalence ratio within a range of volumetric oxygen fraction from 21% to 50%. Hu et al. [94] studied the laminar flame speed of $CH_4/O_2/CO_2$ mixtures at kinetic simulation and ordinary pressure. The laminar flame speed was measured at different equivalence ratio from 0.6 to 1.4 and oxygen percentage from 25 % to 35 % utilizing Bunsen burner. The results showed that at equivalence ratio equal to one, the laminar flame speed of premixed oxy-methane flame reach the highest point. Williams et al. [95] studied the effect of syngas composition and carbon dioxide diluted oxygen on the operability of a premixed swirl combustor. They showed that it is difficult to stabilize flame at less than 22% oxygen fraction. Anderson and Johnsson [96] conducted experiments for air and two O_2/CO_2 cases with various gas mixture concentrations of O_2. The results showed that for Oxygen fraction 21% the fuel burnout is delayed compared to air fired condition. That was attributed to the decreased temperature level. Heil et al. [97] concluded that unstable flames and poor burnout observed at an oxygen fraction equal to 21% of the O_2/CO_2 mixture. The full burnout and stable flames observed at an oxygen fraction equal to 27% and 34%. Aliyu et al. [98] experimentally and numerically studied the characteristics of H_2-enriched-methane oxy-combustion flames in gas turbine combustor. The results showed that enriching methane with hydrogen increases the flame stability. They found the maximum operating equivalence ratio in the gas turbine combustor to be at around 0.85. While it not possible to have a stable flame at an equivalence ratio equal to 0.95. Yu et al. [99] studied numerically and experimentally the combustion characteristics of a premixed combustion with exhaust gas recirculation. The results showed that, as the equivalence ratio increase to 1.0, the NO_x emissions and exhaust gas recirculation reduced due to the reduction in

the maximum flame temperature. Habib et al. [100] experimentally studied the performance of Oxygen-methane combustion in a gas turbine reactor at different operating parameters such as equivalence ratio ranging from 0.5 to 1 and different percentage of CO_2/O_2 in the oxidizer mixture. They found that, when the oxygen fraction in the oxidizer reaches below 25% the flame was affected. The flame blowout occurred when the oxygen fraction reached 21%. Seo et al. [101] studied the effect of various operating parameters on combustion dynamics of a lean premixed flame on a single element swirl injector. When the equivalence ratio ranges between 0.5 and 0.7, unstable flames were observed. Also, when the inlet temperature exceeded 650 K unstable flames were observed.

2.8 Effects of Reynolds Number

The Reynolds number can be expressed as the ratio of the inertial forces to viscous forces.

$$Re = v\, D\, \rho/\mu \tag{1}$$

Where: - v is the flow velocity (m/s), D is the throat diameter (2 cm), ρ is the flow density (kg/m^3) and μ is the dynamic viscosity (Pa.s). Reynolds number has three regimes: - laminar flow, transition flow and turbulent flow [102]. Studies considered Reynolds number is described below.

Guilbert et al. [103] experimentally studied the instabilities of lean premixed combustion using Phase Locked Tomography (PIV). The tomography used in the experiment to analyze the flame front. The experiment discussed the influence of the equivalence ratio (0.65, 0.70, 0.75 and 0.80) at fixed Reynolds number equal to 25000. The results showed that for the equivalence ratio equal to 0.65 and 0.70 no pulse of the flame appears and the flame is found inside the shear layer caused by the step corresponding to the sudden expansion of the channel. For the equivalence ratio, equal to 0.75 and 0.80, the results showed a strong pulse of the flame appears. Carlsson et al. [104] experimentally and numerically studied the flame propagation and quenching of lean premixed turbulent low swirl flames at various Reynolds number from 20,000 up to 100,000 and equivalence ratio equal to 0.62 and the swirl number equal to 0.55. At the burner, Reynolds numbers equal to 20,000 and 30,000 the results show that at the leading edge of the flame, the flame stabilization position, and flame structure are not sensitive to the changing of the burner exit flow velocity but, the flame volume is sensitive to the burner exit velocity. The results also indicated that, the high temperature zone in the flame decreases as the Reynolds number changes from 20,000 to 30,000. It is also observed that when the Reynolds number is higher than 30,000 the flame and the mixing field are less sensitive to the Reynolds number. Baigmohammady et al. [105] experimentally studied the impacts of equivalence ratio, and Reynolds number on methane oxygen premixed flame

dynamics in non-adiabatic cylindrical meso-scale reactor. The results showed that reducing the equivalence ratio at constant Reynolds number and constant geometrical parameters led to different flame regimes in the non-adiabatic reactor. Also, the results showed that increasing the Reynolds number reduce the presence of the flame in the small-scale reactor. At constant Reynolds number ranging from 6700 to 14200 and high pressure turbulent burning velocity, measurements were carried out by Liu et al. [106] a spherical methane air flames were utilized at an equivalence ratio equal to 0.8 in a double chamber, and turbulent combustion facility. The results showed that, at constant Reynolds number, turbulent burning velocities reduce with increasing pressure in a minus exponential manner. Also, the results showed that as the Reynolds numbers increase the turbulent burning velocities increase at any pressure values. Chiu et al. [107] measured a high pressure turbulent burning velocities (S_T) of a lean syngas 35% H_2 and 65% CO at a constant turbulent Reynolds number ($Re_T=u'L_I/\nu$) ranging from 6700 up to 14,200 and elevated pressure equal to 1.3 MPa. Where u' is the root-mean-square turbulent fluctuating velocity and L_I is the integral length scale and ν is the kinematic viscosity. The results indicate that, opposite to most scenarios for turbulent flames at constant Reynolds numbers, the turbulent burning velocities decreases as laminar burning velocities decreases with increasing the pressure in a minus exponential mode. Gobatto et al. [108] studied the impact of the Reynolds number on the isothermal flow field of low

swirl-combustors. The results showed that, the Reynolds numbers affect the flow field of low swirl combustor. More precisely, when the test rig operates at high Reynolds number the velocity peaks are less displaced from the combustor axis. Dellenback [109] found that for un-swirled flows, the mean velocity profiles breakdown to a single curve from Reynolds number equal to 30,000 to 100,000. Syred and Beer [110] concluded that, the Reynold number of 20,000 is sufficient to ensure a very developed central recirculation zone. A comparison between lean air flames and oxy-flames were completed by Watanabe et al. [111]. They observed variations when comparing the air and Oxy-flames at the same Reynolds numbers, swirl numbers, adiabatic flame temperature and equivalence ratio. Jourdine et al. [112] studied the difference between premixed methane oxy-flames and premixed methane air flames in term of stabilization mode at Reynolds number varied from 8500 to 20000. Rashwan et al. [113] studied the flammability limits over a domain of oxygen fractions from 29% to 36%, equivalence ratios from 0.23 to 1.9, and flow Reynolds number from 1100 to 2000. The result showed that, air fuel combustor has more stability limits over all used oxygen fractions. However, they observed that using a mixture of O_2/CO_2 with 36% of oxygen fraction reaches almost 82% of the stability limits range of air-fuel combustor in the used range of Reynolds numbers. Fearn et al. [114] showed a linear increase of the strouhal number (which describe the oscillating flow mechanism) when Reynolds number increased from 155 to 210. Lo et al.

[115] numerically studied the vortex formation processes by using large eddy simulation analysis. They found that the flow behaves similarly at high Reynolds number. However, the large-scale vertical structures are established in finer scale turbulence. Ducruix et al. [116] stated that Reynolds numbers, equivalence ratio, inlet temperature and other flow properties affect the combustion dynamics in swirl-stabilized combustor. Soika et al. [117] studied wire stabilized premixed methane-air flames in a grid generated homogenous turbulent flow field at a constant Reynolds number equal to 87 and 134. The study was completed to identify various burning regimes. Richecoeur and Kyritsis [118] experimentally studied the flame stabilization at low Reynolds number during a non-premixed combustion in curved duct with a diameter in order of magnitude of the premixed flame thickness of the reactants. Bollinger and Williams [119] studied the effect of the Reynolds number in the range from 3000 to 35,000 on the turbulent flame speed. The results showed that the turbulent flame speed is a function of the Reynolds number of the turbulent flow in the burner tube and the tube diameter.

2.9 Effect of Inlet velocity

Many studies discussed the burning velocity and flame speed effect on combustion process. Most of them focused on air-fuel condition [120-122].

Chaparro and Cetegen [123] experimentally studied the Blow-off characteristics of premixed flames under upstream velocity alteration. Three types of flame holders were considered (cone, rod and disk). Propane-air mixtures were used in the experiment at different mixture velocities namely 5, 10 and 15m/s. At 5 m/s velocity, the impact of upstream flame alteration is to enhance flame stability as observed by lower flame blow-off equivalence ratios for the considered flame holders. At 10 and 15 m/s, the rod shape holder provides more flame stability while the cone and disk shape provide less flame stability. Yoon et al. [124] studied the effect of fuel-air mixture velocity on combustion instability. They concluded that combustion instability is reduced at low velocity condition because of fluid dynamical vortex frequency and structure. Papanikolaou and Wierzba [125] studied the stability map of hydrogen-air diffusion flames. They stated that as the co-flow velocity increase, the flame become unstable.

The literature review shows that many works have been completed in oxy-fuel combustion but premixed oxy-combustion is still in research and development stage especially at fixed Reynolds number.

CHAPTER 3

METHODOLOGY

3.1 Description of the Experiments

3.1.1 Specifications of the premixed swirl combustor

The study considers testing fully premixed methane-oxygen flames in a swirl-stabilized gas turbine model combustor under atmospheric combustion conditions. Figure 3 presents an overview of the experiment set-up of the premixed oxy-fuel combustor used in this study. There are three supply lines for the reacting gases including oxygen, carbon dioxide, and methane. The gases are supplied through high-pressure cylinders, and a pressure regulator is fixed at the exit of each cylinder to control the pressure in the supply line. Oxygen and carbon dioxide are introduced to a mixing plenum through two radial tubes, at a vertical distance of 35 mm above the lower base of the test section as per figure 4. In the mixing plenum, fuel and oxidizer gases are mixed before being introduced to the combustor inlet section. Fuel is supplied through a vertical tube, closed at its top end, with 12 radial staggered perforations in three successive planes, at its base within the mixing plenum, ensuring cross flow mixing with the oxidizer mixture. The mixing plenum is of cylindrical shape, 1.0 m length and L/D ratio of ~20, to ensure fully-premixing conditions. The flow volume flow rates of gases are controlled through Bronkhorst-High-Tech mass flow controllers with uncertainty of ±0.5% of maximum

capacity. The controllers are operated through a computer interface to deliver the required flow rates at specific operating condition. A swirler with 55° swirl angle is fixed at the top of the mixing plenum, just upstream of the inlet nozzle and 5 cm below the burner tip as shown in figure 4, to generate the required flow swirl for flame stabilization within the combustor. The swirler is having a swirl number of 0.98 calculated based on the following equation [126]:

$$Sw = \frac{2}{3}\left[\frac{1-\left({}^{D_{cb}}/_{D_{in}}\right)^{3}}{1-\left({}^{D_{cb}}/_{D_{in}}\right)^{2}}\right]\tan(\alpha_{sw}) = 0.98 \quad (2)$$

Where α_{sw} is the blade angle, D_{cb} the center-body diameter and D_{in} is the inlet tube diameter. An inlet nozzle, sitting on the swirler and tightened in place by bolts, with a diameter of 2 cm is utilized to accelerate the flow at combustor inlet with the required velocity and ensure keeping the swirl intensity of the flow until reaching the combustion chamber. The nozzle is of convergent-divergent design with 30° convergent angle. The nozzle is of 45° divergence angle to inhibit sudden expansion of the reactants into the combustion chamber. The combustion chamber is optically accessible quartz tube opened to the atmosphere having an inside diameter of 63.5 mm and length of 30 cm. To avoid flashback inside the mixing plenum, a solid conical projection is placed at inlet nozzle throat [127]. An emergency shut-off valve is affixed on the fuel delivery tube to cut the fuel supply and shutdown the system in case of flashback. To record the changes in flame macrostructure, a digital camera with shutter speed of 1/60 s is used to capture the images of the selected flames. Temperature measurements are conducted using an R-type (PtRh13%-Pt) thermocouple connected to a readout device with a RS232 cable for direct data logging.

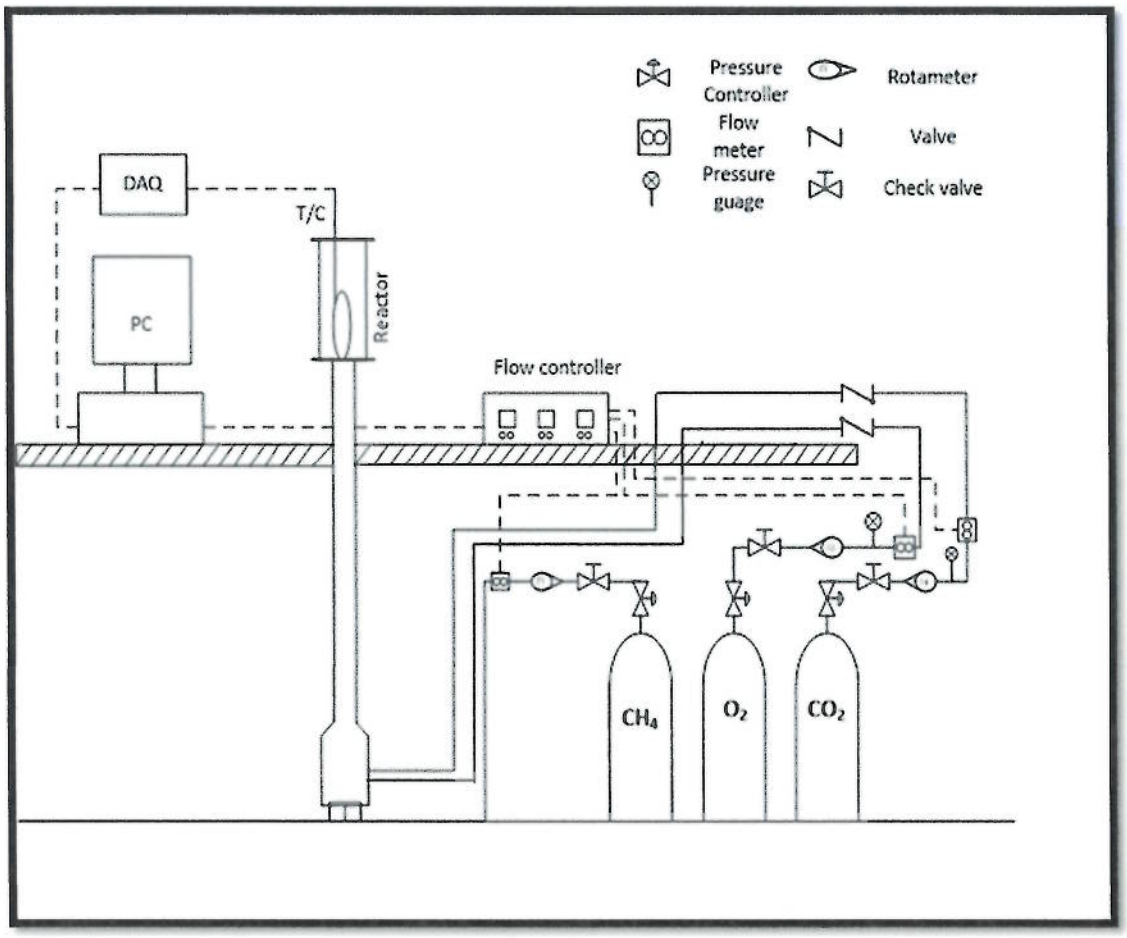

Figure 3 Schematic diagram showing the experimental setup.

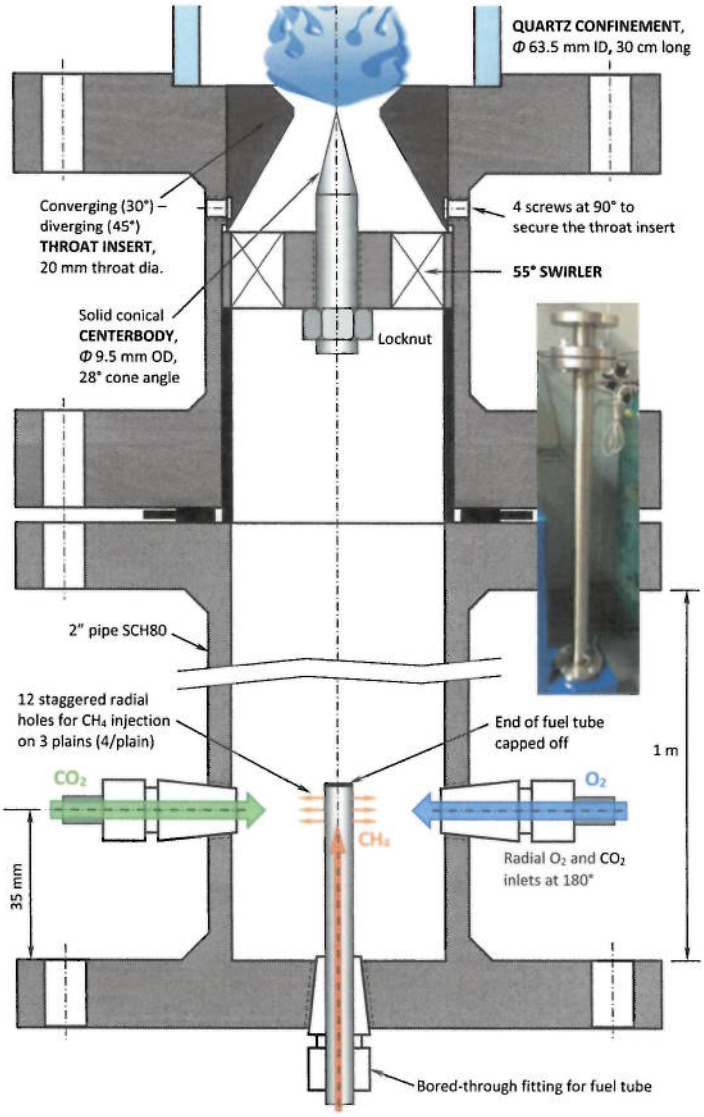

Figure 4 Detailed design description of the considered gas turbine model combustor.

3.1.2 Operating conditions and approach

Three sets of experiments were performed in this study, each at fixed *Re*, in a swirl-stabilized gas turbine model combustor under premixed oxy-combustion conditions. The considered three *Re* values are namely 7,000, 9,000 and 11,000. Methane (CH_4) is used as a fuel, and a mixture of oxygen (O_2) and carbon dioxide (CO_2) is used as oxidizer. At *Re* of 7,000, the stability limits are obtained through running the combustor at fixed U_{in}

and variable OF (from 29% to 70% by volume) and φ (from 0.2 up to 1.0) until the flashback and blow-out limits occur. The values of φ and OF at these limits are then recorded on the stability map. Then, U_{in} is changed at the same Re of 7,000and the same procedure was repeated. At Re of 7,000, the full stability map is obtained considering the combustor operation at four values of U_{in}, namely 3.7, 4.0, 4.3 and 4.6 m/s. Same approach is followed to obtain the full stability maps at the other two Re values, 9,000 and 11,000. The stability map at Re of 9,000 is obtained for combustor operation at four values of U_{in}, namely 4.8, 5.2, 5.6 and 6.0 m/s. Similarly, the considered inlet velocities at Re of 11,000 are 5.8, 6.3, 6.8 and 7.3 m/s. Detailed description of the experimental procedure and testing method is provided in previous work [128], considering the same experimental set-up.

The obtained stability limits for the considered three sets of experiments are plotted on a 2-D stability map as function of φ and OF. The maps are presented on contour plots of T_{ad}, U_{in} and PD of the combustor to configure the physics of flashback and blow-out limits. These contours are calculated as function of φ and OF. Same procedure, like in the previous work [128], is followed in the present study to calculate T_{ad} as function of the operating φ and OF. The PD of the combustor in MW/m^3/bar is calculated using the following equation:

$$PD = \frac{\dot{m}_{CH4} \times HV_{CH4}}{P \times V_C} \tag{3}$$

Where $\dot{m}_{CH4}$is the mass flow rate of CH_4 calculated based on the operating φ and OF in kg/s, HV_{CH4} is the standard heating value of CH_4 in MJ/kg, P is the operating pressure in bar and V_C is the volume of the combustion chamber.

In addition to stability maps, the changes in flame macrostructures are recorded through capturing flame images to identify the different flame transition modes from stable operation toward the stability limits. Also, the effects of the different operating parameters OF, φ, U_{in}, T_{ad} and Re on shape and stability of the different flames are investigated.

CHAPTER 4

RESULTS AND DISCUSSIONS

4.1 Combustor stability mapping

In this section, combustor stability mapping is presented under fixed *Re* operation considering three sets of stability maps. The three sets of stability maps present the stability limits as function of φ and *OF* on the contour plots of U_{in}, T_{ad} and *PD* of the combustor, respectively. For each set, three stability maps are presented, each at fixed *Re*. The considered *Re* values for the operation of the combustor are 7,000, 9,000 and 11,000. The combustor stability mapping is determined by recognizing the blow-out and flashback limits of the flames at fixed *Re* by fixing U_{in} and varying φ and *OF* until flashback and blow-out limits are obtained and repeating the procedure under different operating U_{in}. At *Re* of 7,000, the stability limits are recorded considering combustor operation at four values of U_{in}, namely 3.7, 4.0, 4.3 and 4.6 m/s. the corresponding values of U_{in} while combustor operation at *Re* values of 9,000 and 11,000 are; 4.8, 5.2, 5.6, 6.0 m/s and 5.8, 6.3, 6.8 and 7.3 m/s; respectively.

4.1.1 Stability maps on a background of corresponding U_{in} at constant inlet *Re*

Figure 5(a), figure 5(b), and figure 5(c) present the first set of stability maps on the contour plots of the corresponding U_{in} for different constant inlet *Re*. Figure 5(a) presents the stability map at *Re*=7,000, figure 5(b) presents the stability map at *Re*=9,000, and

figure 5(c) presents the stability map at Re=11,000. The areas above the flashback line and below the blow-out line present unstable flame operation zone, while the area between the two lines presents the stable operability window of the flame. For fixed Re operation, the flashback lines best fit with a second order curve with negligible differences in the slope. However, the type of the curve fit equation and slope are altered while varying the operating Re, as per figure 5(a), figure 5(b), and figure 5(c). The curve fit equation is altered from the second order form to the exponential form while varying Re from 7,000 to 9,000 and getting back to the second order form with different slope while operation at Re of 11,000. For all curve fit lines, the R^2 (coefficient of determination) values are close to 1.0 indicating reasonable curve fit equation.

The results in figure 5(a), figure 5(b), and figure 5(c) show almost identical flashback conditions at all operating Re values indicating insignificant effect of the operating Re on the flashback limit of the generated flames. However, Re has a role in determining the blow-out limit of the generated flames depending on the U_{in}. This indicates that the rate of reaction kinetics near flashback is a more relevant parameter than the flow dynamics (associated with change in Re) for determining the flame speed and, consequently, the flashback limit. On the other hand, near blow-out limit, the stability of the flame depends mainly on the generated flow dynamics within the combustor, which control flame anchoring under lean operating conditions. The lines of flashback and blow-out do not follow constant U_{in} trends as shown in figure 5(a), figure 5(b), and figure 5(c). However, at any operating Re, increasing U_{in} reduces the operability window of the flame and shifts the flashback limit to the leaner side. For fixed U_{in} operation, flashback and blow-out phenomena are mainly function of the reaction time scale (flame speed) based on the

definition of the Damkohler number [129, 130]. Increasing the *OF* in the oxidizer mixture results in improved flame speed [131, 132]. Increasing U_{in} at fixed *Re* requires the increase of the *OF* in the oxidizer mixture in order to have a stable flame operation. This should result in improved flame speed which overcomes U_{in} at lower operating equivalence ratio causing flashback of the flame. As a matter of fact, U_{in} is a major controlling parameter of premixed flame stability governing the size and strength of the ORZ.

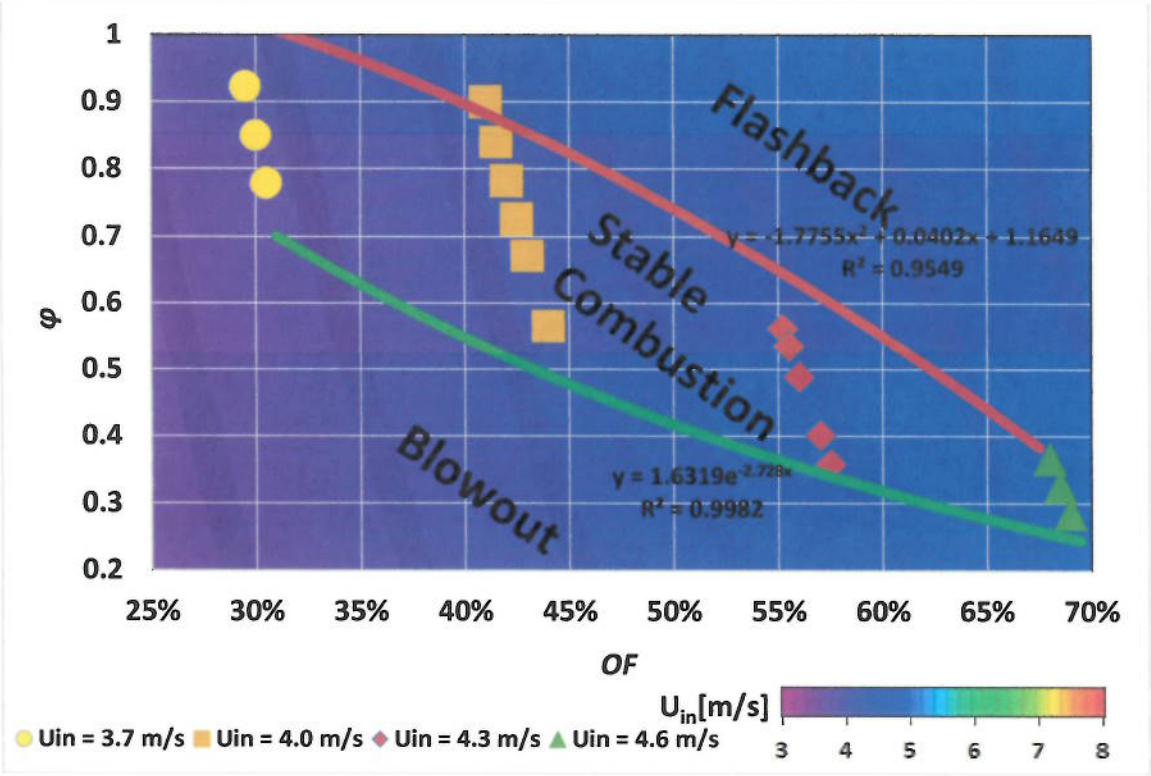

Figure 5(a) Stability map on a background of corresponding U_{in} at *Re*=7,000.

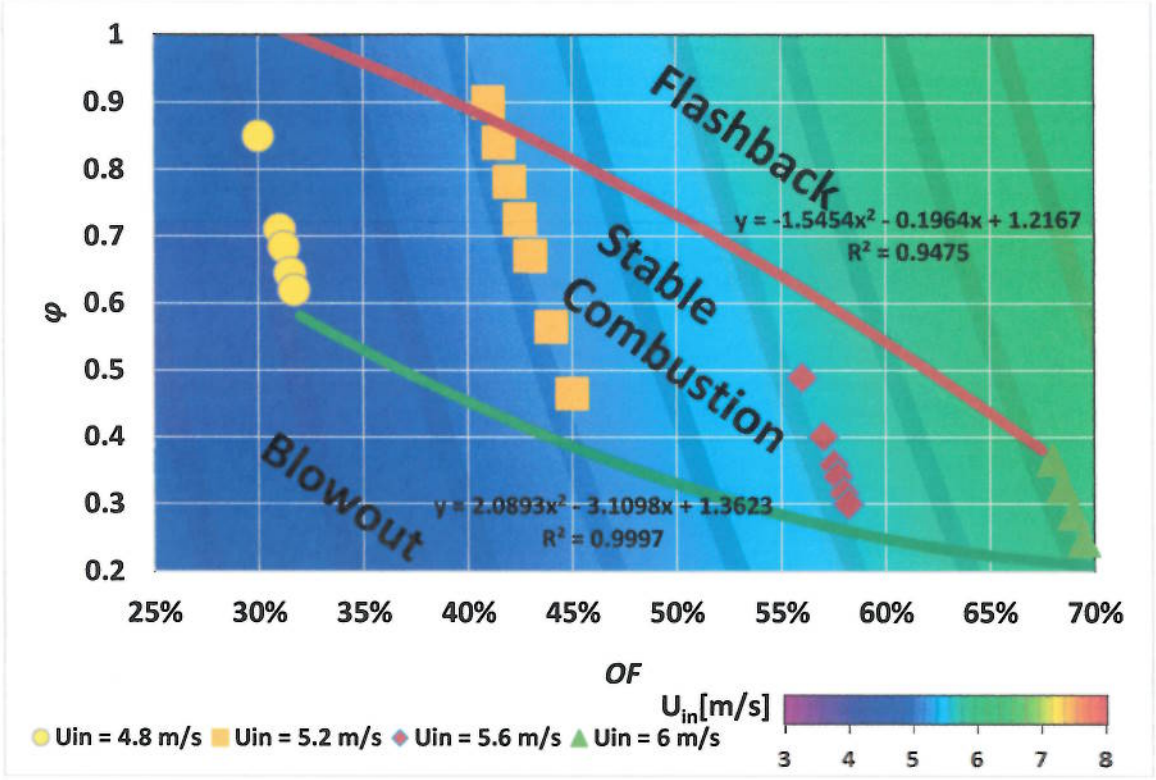

Figure 5(b) Stability map on a background of corresponding U_{in} at Re=9,000.

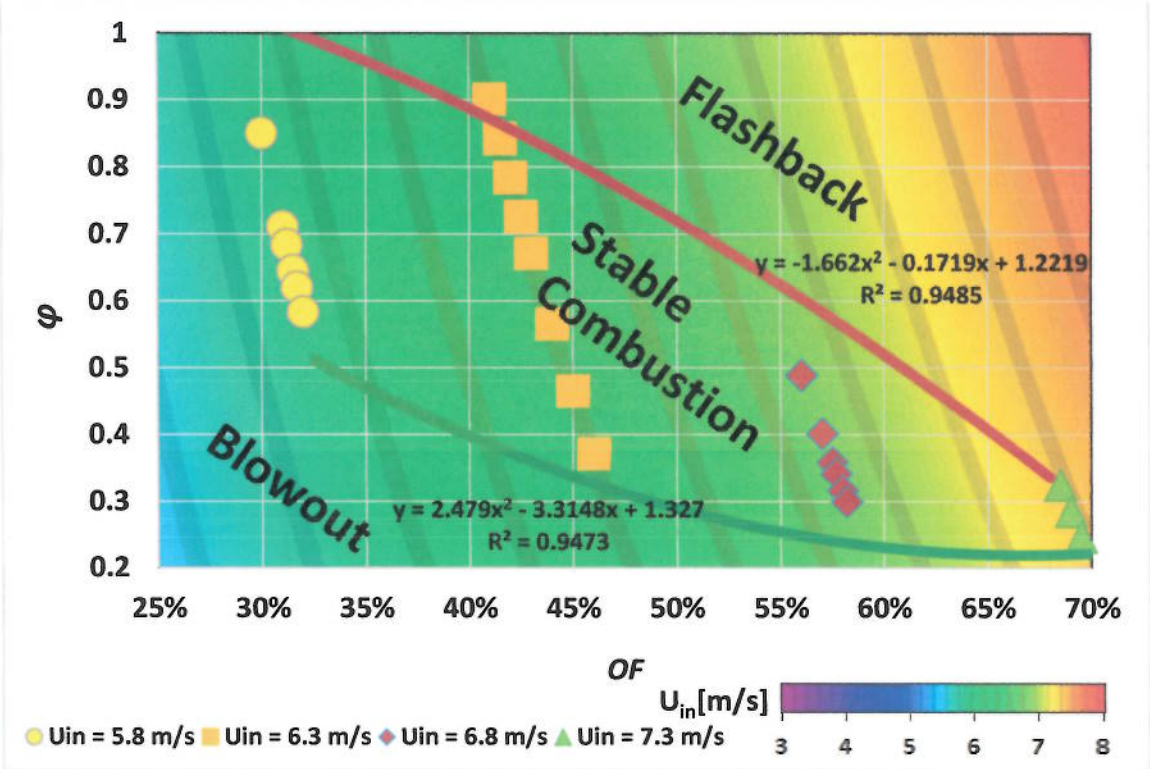

Figure 5(c) Stability map on a background of corresponding U_{in} at Re=11,000.

4.1.2 Stability maps on a background of corresponding combustor *PD* at constant inlet *Re*

Figure 6(a), figure 6(b), and figure 6(c) show the same stability maps plotted on a background of combustor *PD* trying to configure if the static stability limits correlate with the combustor *PD* under fixed *Re* operation. Stability maps are also presented in figure 6(a) at *Re* = 7,000, figure 6(b) at *Re* = 9,000, and figure 6(c) at *Re* = 11,000. The contour plots of *PD* in figure 6(a), figure 6(b), and figure 6(c), for all operating *Re* values, do not correlate with the line presenting the flashback limit. However, for all operating *Re* values, the line presenting the blow-out limit fits well with a line of constant *PD*. For the three operating *Re* values, the flame blows-out at the same operating combustor *PD*, about 3.0 $MW/m^3/bar$. On the other hand, the combustor *PD* at flashback increased from about 5.0 $MW/m^3/bar$ at Re of 7,000 to about 7.0 $MW/m^3/bar$ at Re of 11,000. These results indicate that the fuel mass flow rate, based on a given size of the combustor, plays a key role in controlling flame stability near the lean blow-out limit, and should not drop below a certain value to avoid flame blow-out if the flow dynamics within the combustor are kept similar by keeping the same operating *Re*.

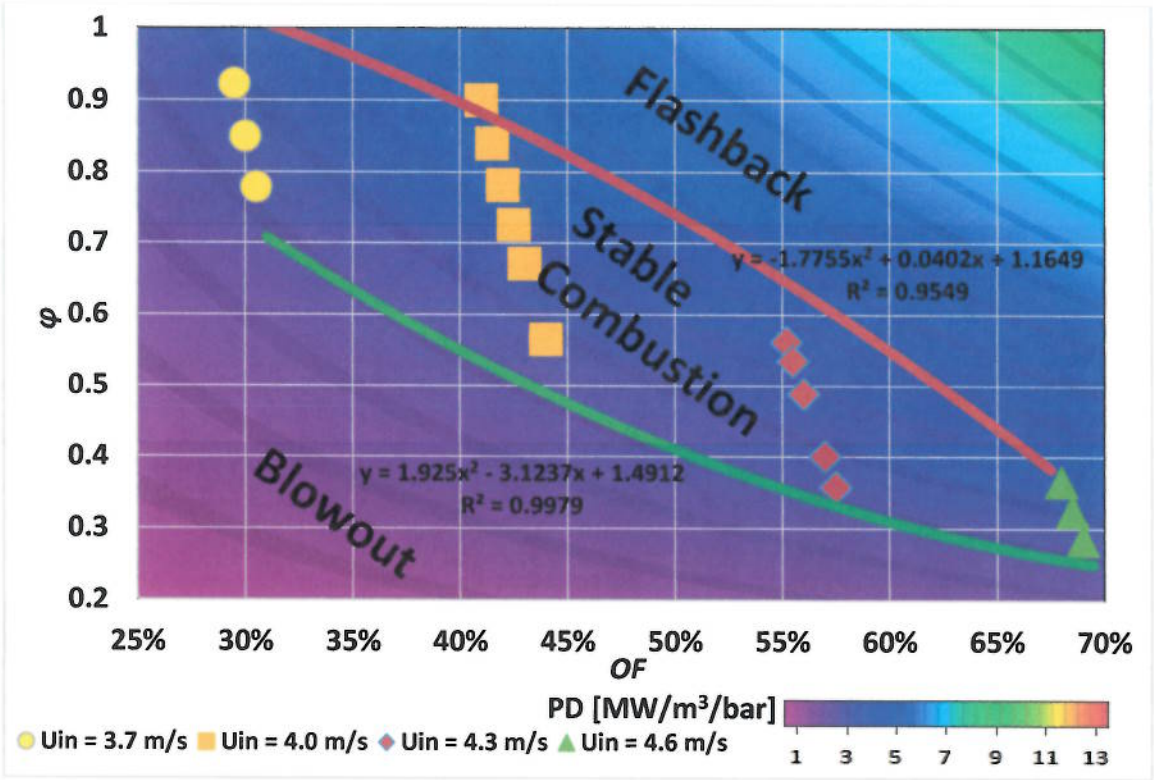

Figure 6(a) Stability map on a background of corresponding *PD* at *Re*=7,000.

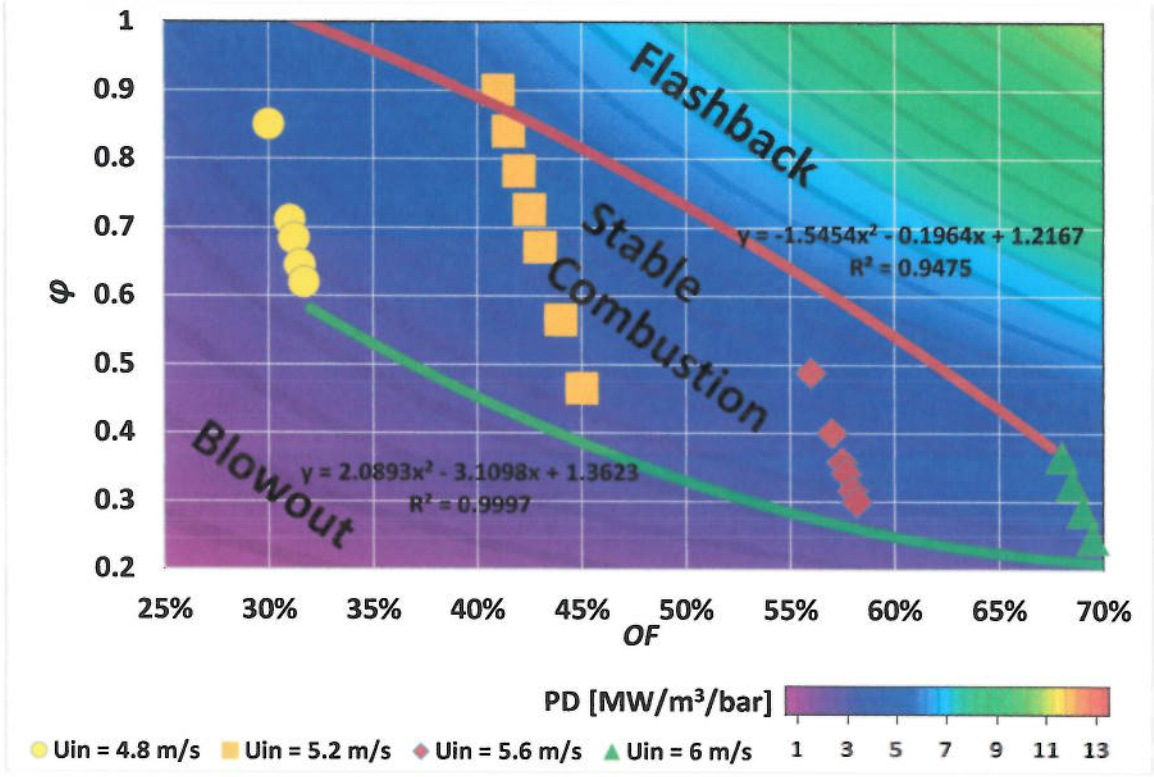

Figure 6(b) Stability map on a background of corresponding *PD* at *Re*=9,000.

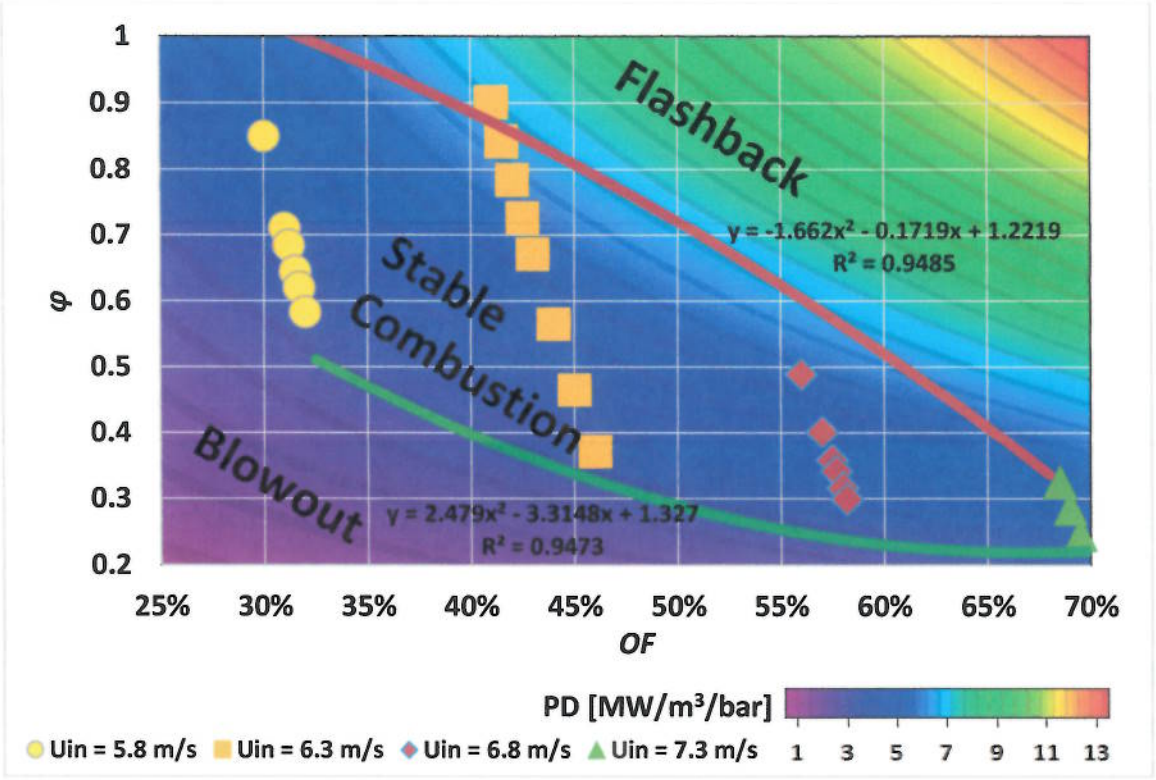

Figure 6(c) Stability map on a background of corresponding *PD* at *Re*=11,000.

4.1.3 Stability maps on a background of corresponding combustor T_{ad} at constant inlet *Re*

The stability limits are also plotted on a background of the contours of T_{ad} for the three operating *Re* values as presented in figure 7(a), figure 7(b), and figure 7(c). As per these figures, the plots do not show direct link between T_{ad} and flashback and blow-out phenomena under fixed *Re* operation. Interestingly, based on previous work on the same combustor set-up done by Abdelhafez et al. [128], the results showed that both flashback and blow-out lines are following lines of fixed T_{ad} but under fixed U_{in} operation. Which means that T_{ad} is the most relevant parameter controlling both flashback and blow-out phenomena while operating under fixed U_{in} [128]. However, for operation under fixed *Re*, the fuel mass flow rate is the most relevant parameter controlling flame blow-out

limit. While the flash back limit under fixed *Re* operation is mainly controlled by the rates of reactions kinetics, based on operating φ and *OF*. In addition, it is observed that it is not possible to sustain premixed oxy-methane flames in the ranges of *OF* below 29% and above 70%. These ranges match with the reported results in previous work on oxy-flames stabilized over a perforated plate burner [113].

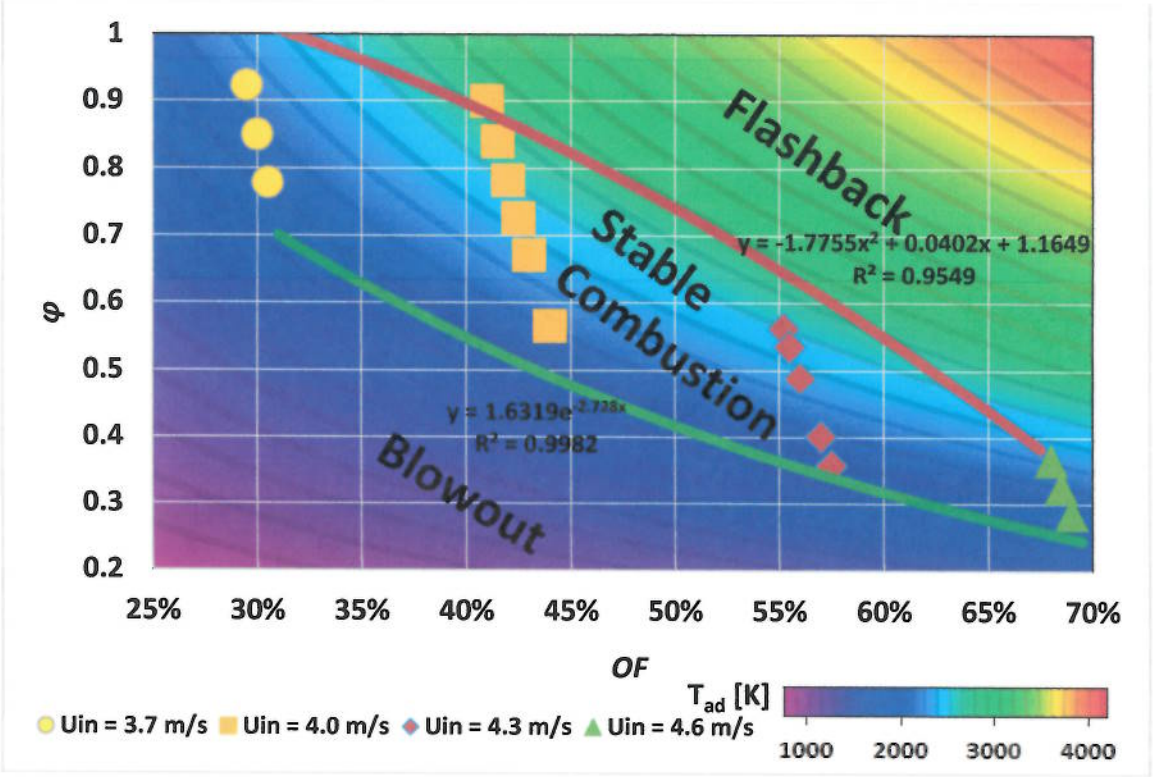

Figure 7(a) Stability map on a background of corresponding T_{ad} at *Re*=7,000.

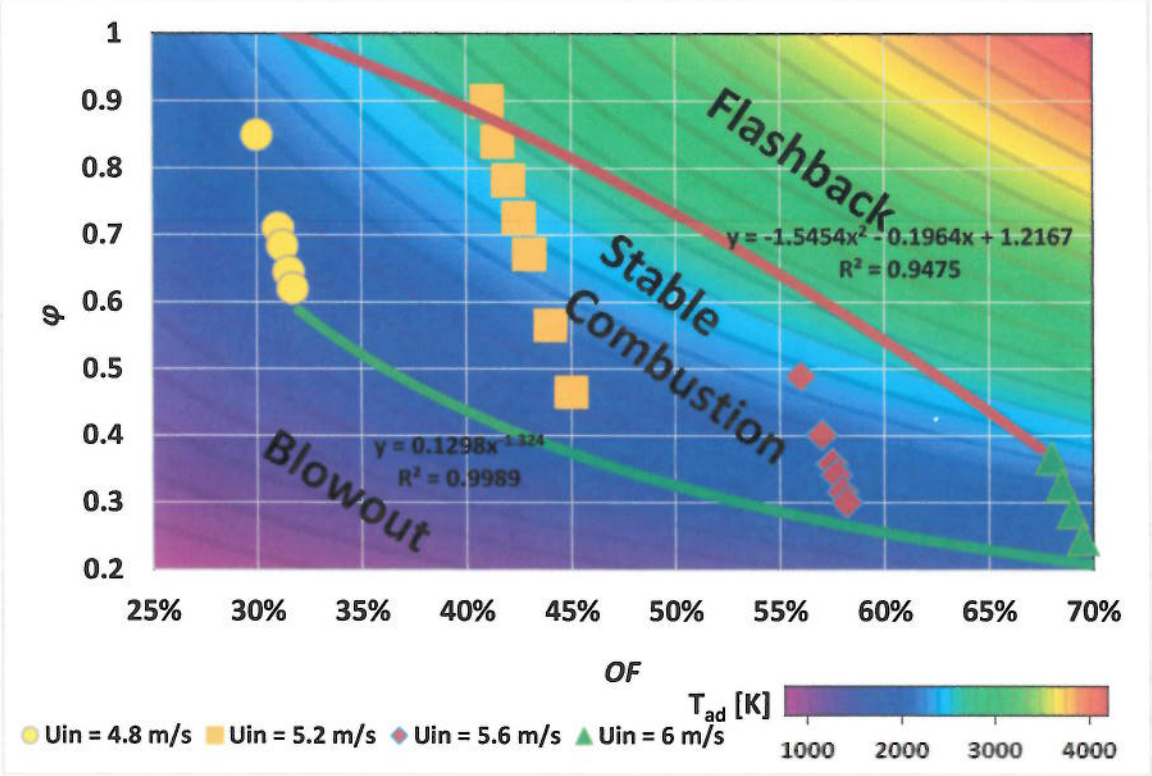

Figure 7(b) Stability map on a background of corresponding T_{ad} at Re=9,000.

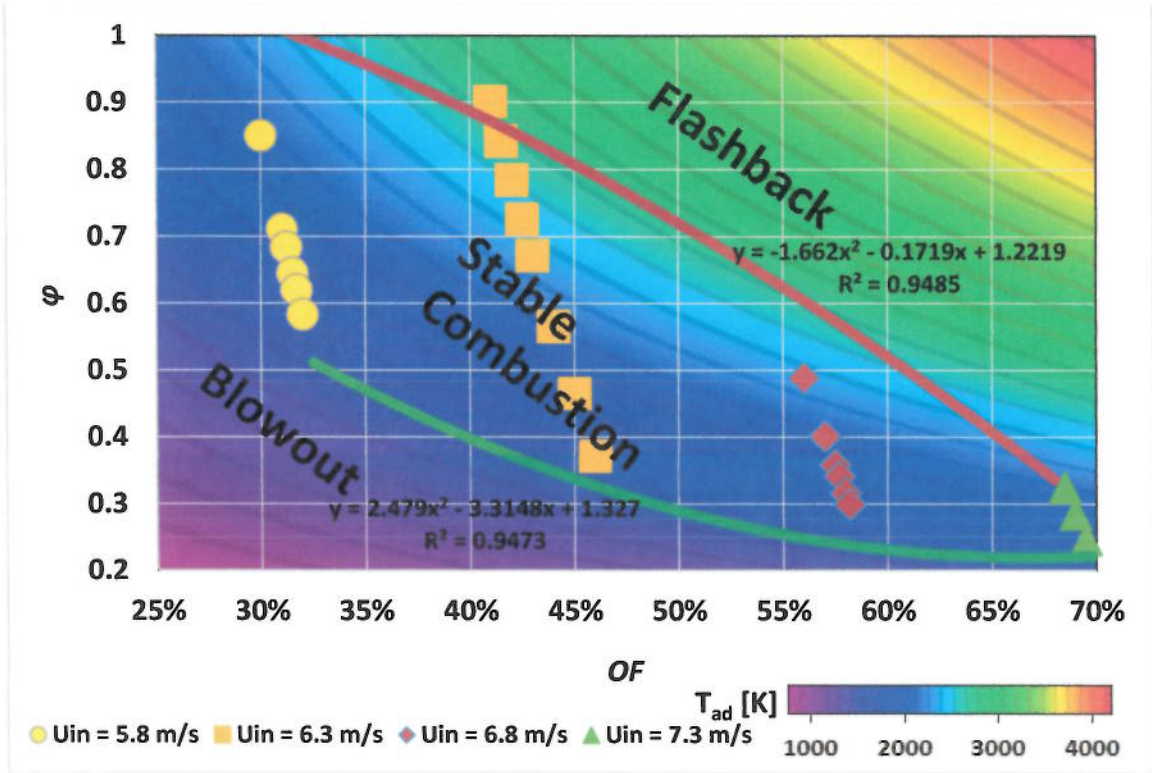

Figure 7(c) Stability map on a background of corresponding T_{ad} at Re=11,000.

4.2 Effect of *Re* on flame stability

To have clearer comparison of stability limits under different operating *Re*, the lines presenting the flashback limits under the different operating *Re* are presented in one figure 8. As per figure 8, the lines presenting the flashback limits are almost identical under all operating *Re*. The results in figure 8 confirm the finding based on the above discussion that *Re* has insignificant effect on determining the flashback limits of the test premixed flames under oxy-combustion conditions. As a matter of fact, flashback occurs when the flame speed of the reacting mixture exceeds U_{in}. In addition, while varying the *Re* during the experiments, the value of U_{in} is accordingly varied, which means that the flame speed at which flashback occurs is also varied. This means that the flashback phenomenon is mainly controlled by the rates of reactions kinetics, which control the flame speed based on operating φ and *OF*. Amato et al. [52] reached a similar conclusion on the stability limits of premixed oxy-methane flames.

Similarly, the lines presenting the blow-out limits under the same operating conditions are presented in figure 9 trying to explore the effect of *Re* on flame static stability limits. As per figure 9, increasing the *Re* widens the operability range of the flame by shifting the blow-out limit toward leaner conditions. This may be attributed to the improved flame anchoring under such limiting operating conditions due to the improved flow swirl in the ORZ because of the corresponding increase in U_{in} at higher operating *Re*. These results indicate a key role of the flow dynamics (mainly function of U_{in}) within the combustor for controlling flame lifting and reattachment encountered before the blow-out of the flame.

To have more insight on the mechanism of flame blow-out, tracing visually, through captured flame images was accomplished, to study the changes in flame stabilization behavior from the flashback limit to the blow-out limit. The combustor has run under fixed Re and fixed U_{in} while varying φ and OF from flashback toward blow-out and the process is repeated for different values of U_{in} under the same Re. Then, the complete set is repeated under different Re. It is found at each operating U_{in} that there is an operating φ at which there is a transition in the flame stabilization mode from being stabilized in the ISL to be stabilized in the ORZ. It is found that this transition is associated with the onset of thermos-acoustic instability and occurs prior to flame blow-out limit. The values of φ at which this transition occurs are presented in figure 10 as function of U_{in} at different operating Re. As shown in the figure, the flame transition occurs at higher velocities for higher operating Re but almost at the same φ indicating insignificant effect of Re on flame stability. At fixed Re, the results in figure 10 show that the increase of U_{in} retards the flame transition toward leaner conditions, closer to the lean blow-out limit. This may be attributed to the enhanced flow recirculation in the ORZ at higher U_{in}. The slopes of the curves in figure 10 are high indicating a leading role of U_{in} in controlling flame stabilization behavior. The transition can occur at different T_{ad} and flame speed. This flame transition from the ISL to the ORZ is mainly governed by the extinction strain rate if similar flow conditions (similar U_{in}) are imposed in the ORZ [126]. The main dimensionless parameter characterizing the flow in the ORZ is the Strouhal number ($St=f. D_{in}/U_{in}$). This number is function of the azimuthal spinning frequency in the ORZ (f), U_{in} and inlet diameter (D_{in}) and independent of the flow Re. These results can lead us to an

important implication that U_{in} is a more relevant parameter choice than Re for the control of the flow conditions in the ORZ and flame stability.

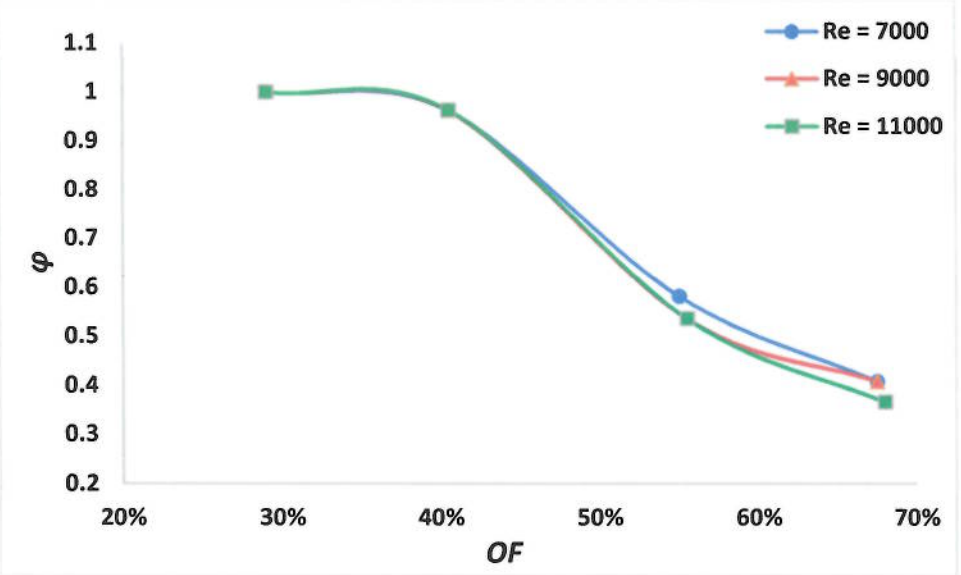

Figure 8 Obtained flashback limits at different inlet Re.

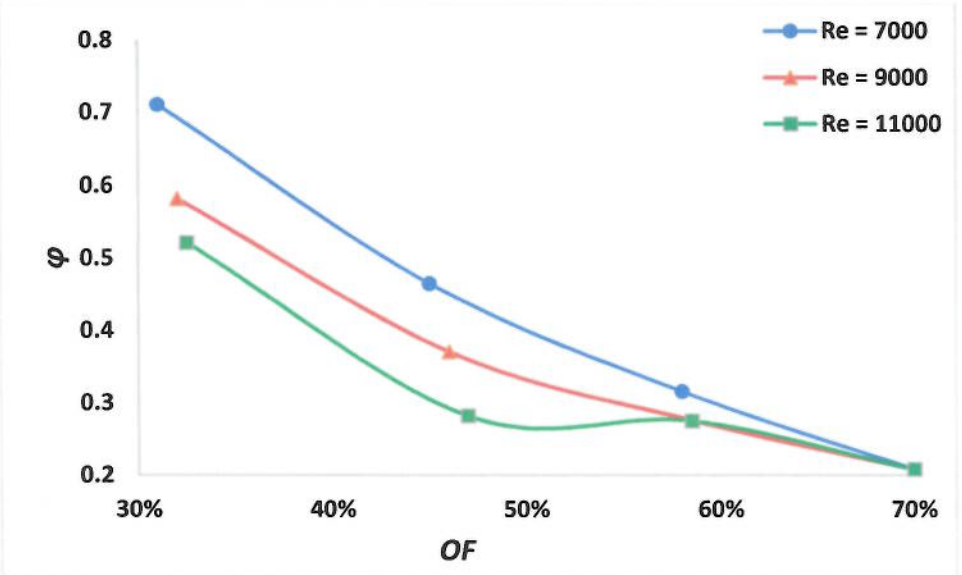

Figure 9 Obtained blow-out limits at different inlet Re.

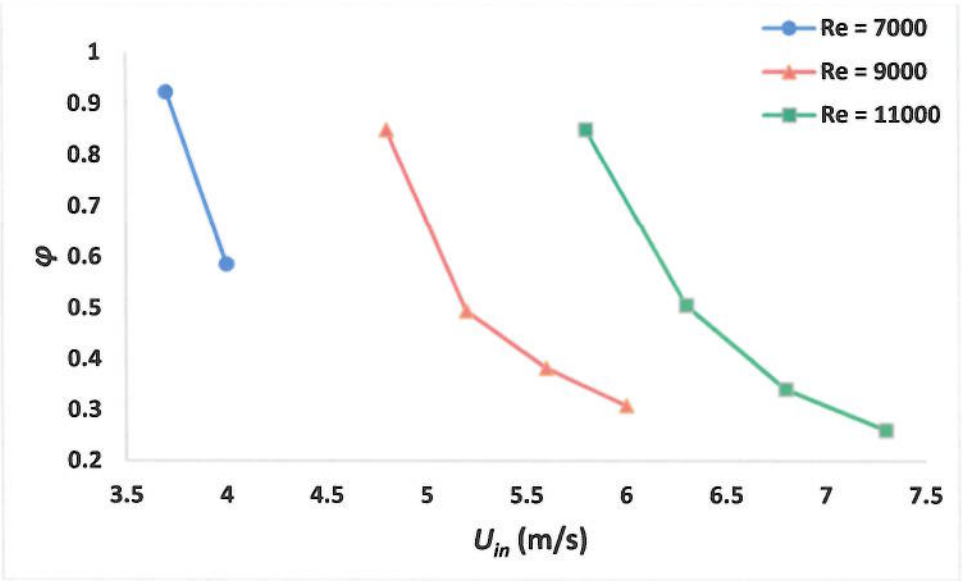

Figure 10 Equivalence ratio at the onset of flame transition from the ISL to the ORZ as function of U_{in} for different operating Re.

4.3 Stability and changes of flame macrostructure

In this section, I will try to explain the modes of flame stability and transition from one mode to another and the analysis of the changes of flame macrostructure.

4.3.1 Analysis of flame stability and macrostructure at fixed U_{in}, Re, and T_{ad}

In figure 11, three sets of flame images were analyzed, under different operating Re, captured at steady state conditions. Each set of flame images is captured under fixed Re and fixed U_{in} while varying OF and φ. The operating Re is increased from one set to another through increasing U_{in} and keeping the same OF and φ for the corresponding flames. The results confirm that the operation under higher Re can extend the flame operability limit to leaner conditions before flame blow-out. At Re values of 9,000 and 11,000, the flame encountered a lifted unstable operation mode before being blown-out; however, at low operating Re of 7,000, the flame encountered blow-out directly without

being lifted-off. The flames at higher Re can sustain better flame anchoring under extra lean conditions compared to those at lower Re. This may be attributed to the improved circulation in the ORZ at higher U_{in} corresponding to higher Re operation. Comparing the corresponding flames (with the same OF and φ, i.e. same T_{ad}) in the three sets of flame images in figure 11 indicates that flames of the same T_{ad} do not necessarily have the same flame macrostructure; flames at higher Re (higher U_{in}) have bigger flame size. This indicates that T_{ad} alone does not have a key role for controlling flame macrostructure and stability. Trying to specify the controlling parameters of flame macrostructure, the flame images were compared while fixing both, the flow Re at 9,000 and T_{ad} at 2000 K, as shown in figure 12. The results showed that similar flame macrostructures can be obtained while fixing one flow characteristic parameter (Re) and one flame characteristic parameter (T_{ad}). Similar conclusion in a previous study on the same combustor set-up using the same fuel type is approached [128]; however, the similar flame macrostructures were obtained while fixing both, U_{in} and T_{ad}.

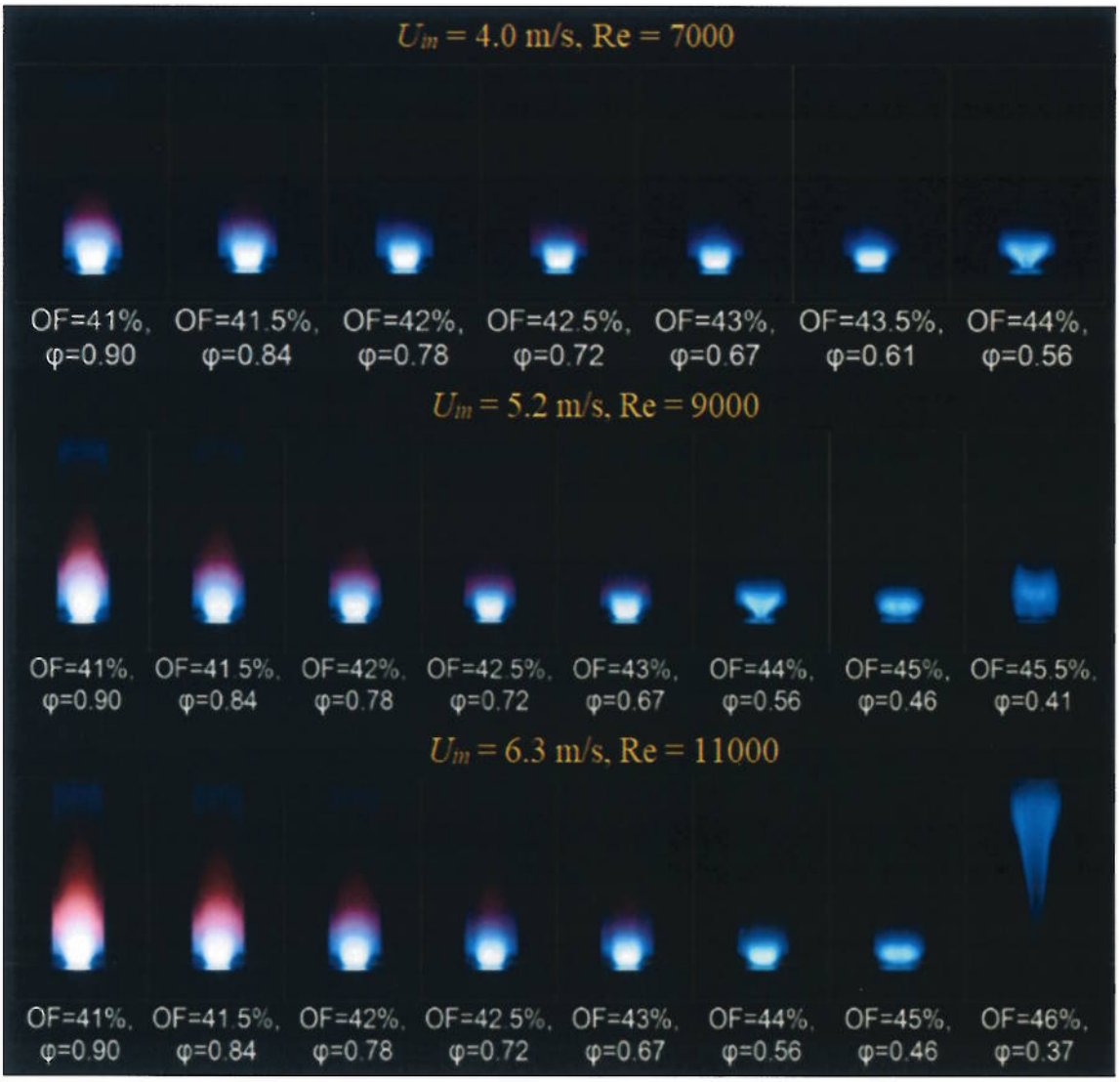

Figure 11 Flame macrostructure at fixed U_{in} from near flashback (left) to near blow-out (right) limits for different inlet *Re*.

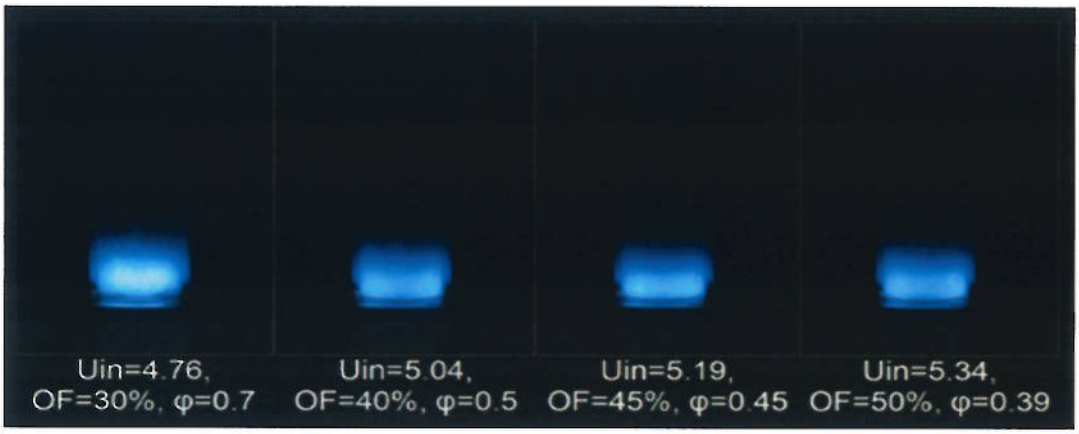

Figure 12 Comparison of flame macrostructures while fixing both the flow *Re* at 9,000 and T_{ad} at 2000 K

4.3.2 Analysis of flame stability and macrostructure at fixed φ as a function of *OF* for different inlet *Re*

To explore the effect of *OF* on flame macrostructure and stability, I tried to compare the flame images in the stable operation zone while keeping φ unchanged (φ=0.5) as presented in figure 13. The figure presents three sets of flame images, each at fixed *Re*. The results show significant effect of *OF* on flame macrostructure and color. Increasing *OF* results in more compact and violent strong flame with brighter color, thus, indicating improved reaction kinetics. This is due to the associated increase in flame speed. As per the measurements of flame speed of oxy-methane flames by Kutne et al. [40], the flame speed is raised by a factor of 2.4 when the *OF* is increase from 30% to 40% in the oxidizer mixture. Increasing the *OF* moves the flame upstream toward the burner throat, as per figure 13, indicating higher flame speed. Thus, *OF* has a major controlling role on the flame macrostructure and stability. At the same operating φ, *Re* seems to have minor effect of flame macrostructure as per figure 13.

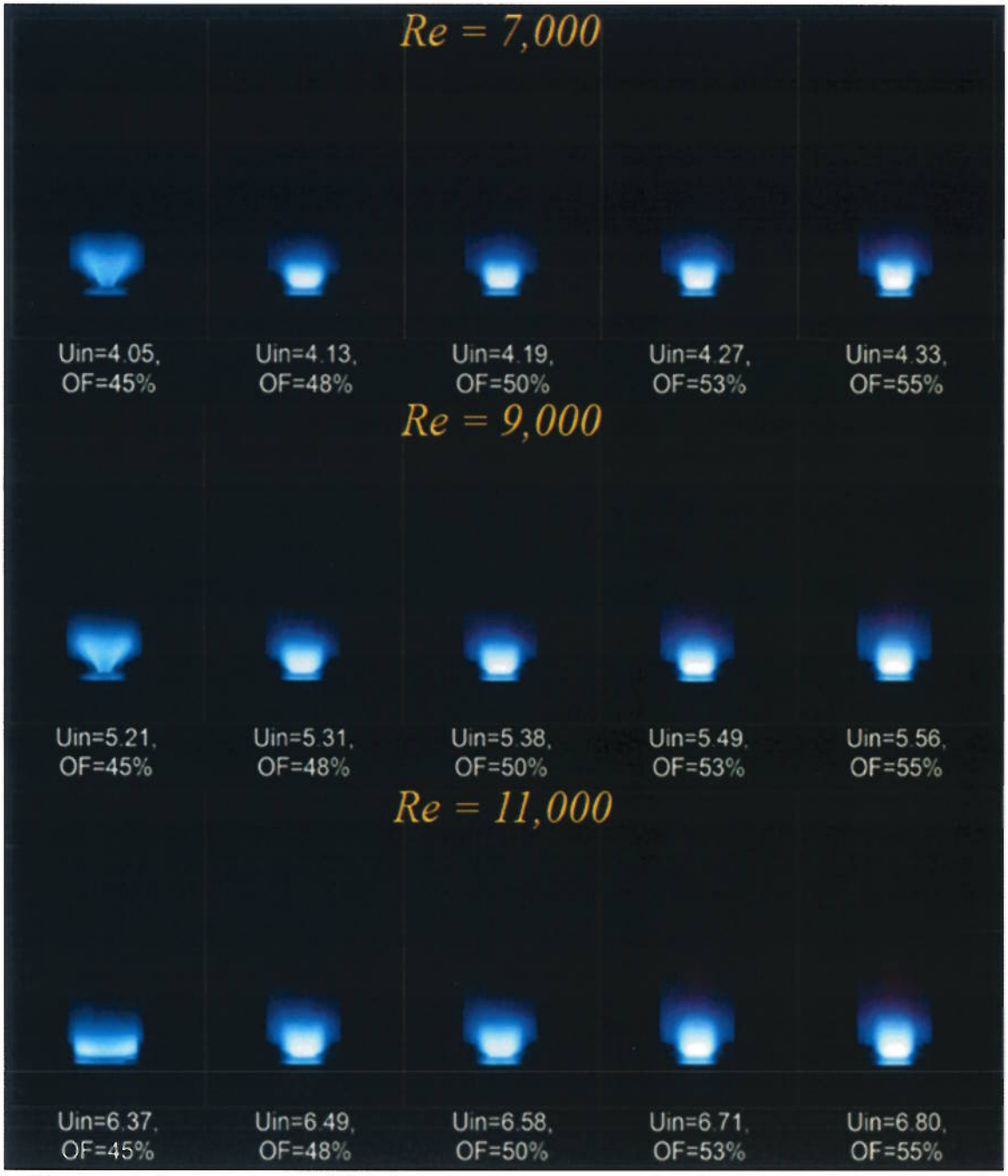

Figure 13 Comparison of flame macrostructures at fixed φ of 0.5 as function of *OF* for different inlet *Re*.

4.3.3 Analysis of flame shapes near blow-out limit and flashback limit at different inlet *Re*

Flame macrostructures near blow-out and flash back limits are presented in figures 14 and 15, respectively, to explore whether the flames hold fixed macrostructure near blow-out or flashback limits under fixed *Re* operation. Three sets of flame images are presented in each figure; each set is recorded at fixed *Re*. The results in both figures show that the flames do not hold fixed macrostructure either near flashback or near blow-out limits. The flames at lower *Re* blow-out without being lifted and have the V-shape of varied size near blow-out. While at higher *Re*, the flames encounter successively stabilization in the ORZ followed by lift-off before being blown-out. While increasing U_{in} under higher *Re* operation, the flame lift-off mode is skipped, and the flame become stronger and shorter before the flame blow-out. Thus, increasing U_{in} under higher *Re* operation helps better flame anchoring near blow-out limit as presented in the bottom set of flame images in figure 14. Near the flashback limit, the flame macrostructure is almost of V-shape of varied size and color as shown in figure 15. The flame macrostructure depends on the reacting mixture composition and reaction kinetic rates which determine the flame speed near the flashback limit. Increasing U_{in} at constant *Re* reduces the flame height and increases the noise level due to increased flame speed near the flashback limit.

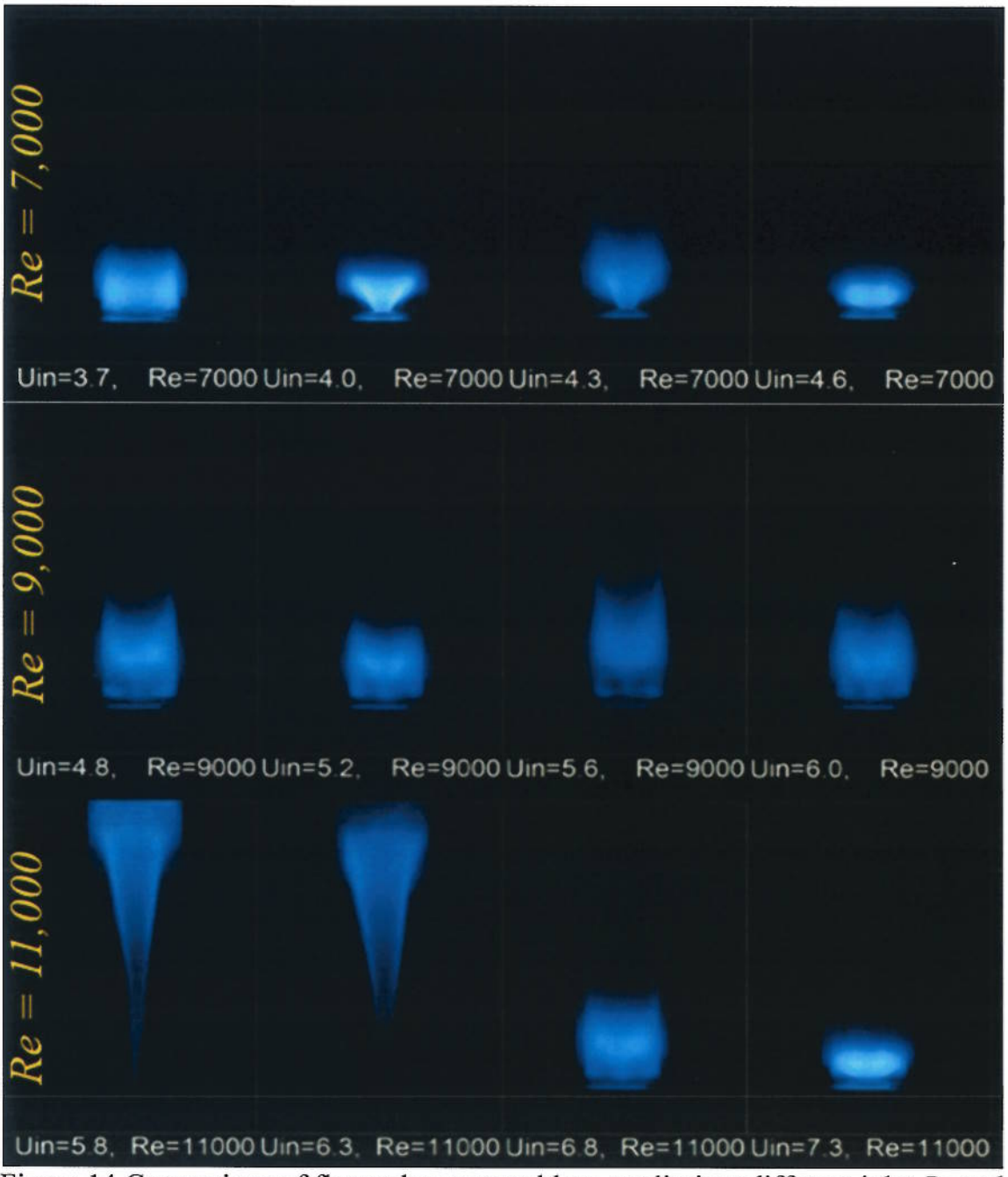

Figure 14 Comparison of flame shapes near blow-out limit at different inlet *Re* and $U_{in.}$

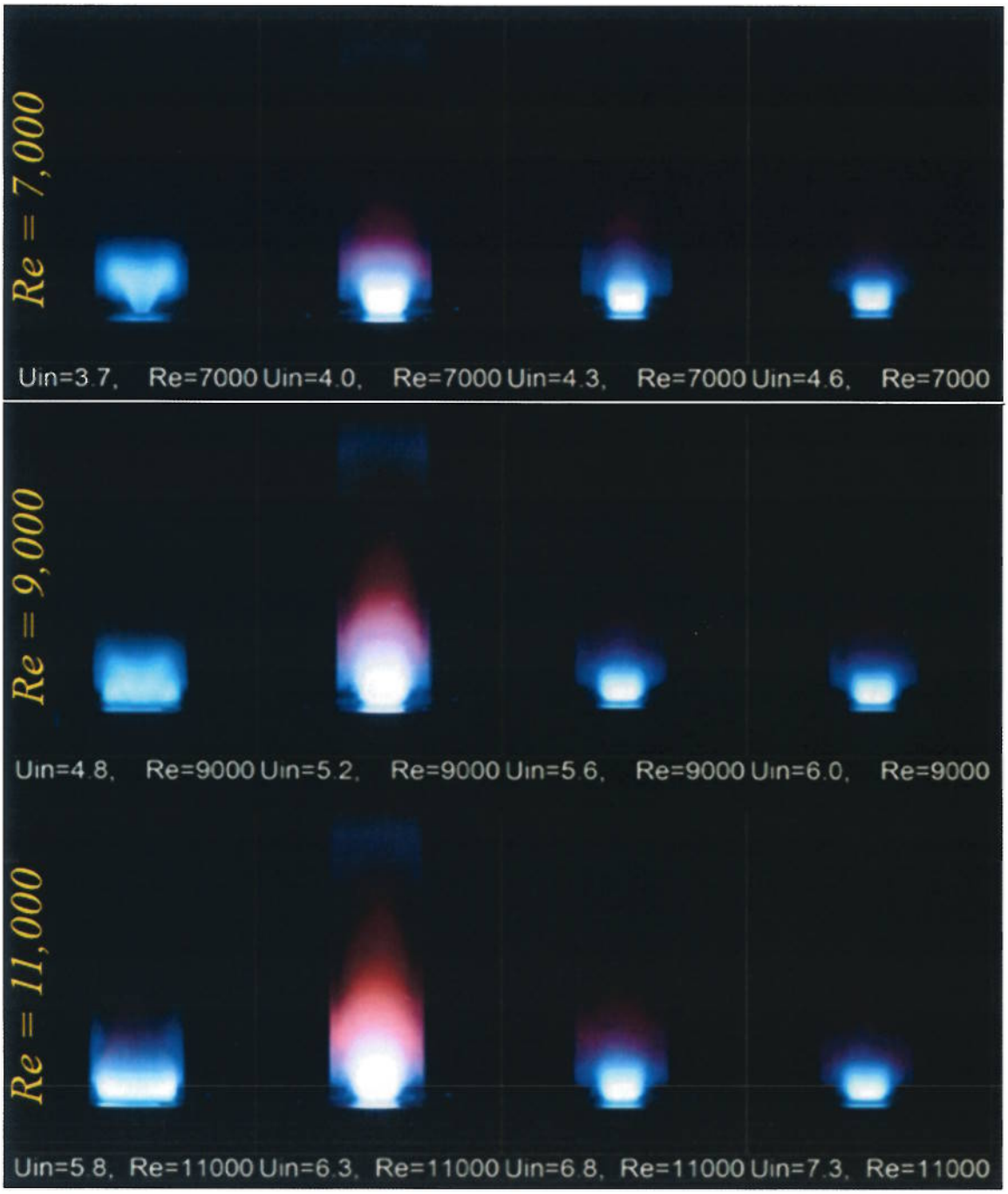

Figure 15 Comparison of flame shapes near flashback limit at different inlet Re and U_{in}.

4.3.4 Analysis of flame macrostructure at fixed *Re*, equivalence ratio, and *OF*

Figure 16 show flame images at constant Reynolds number 7000 and constant velocity 4.12 m/s. The images were captured at different oxygen fraction (45%, 45.7%, 46.4%, and 47.2%) and different equivalence ratios 0.750, 0.675, 0.6 and 0.525. The results indicate that decreasing the oxygen fraction and increasing the equivalence ratio provide more compact and strong flame. Figure 17 and figure 18 were taken to analyze deeply the effect of oxygen fraction and equivalence ratio on flame shape and stability. Figure 17 shows the flame shape at constant equivalence ratio 0.525 at different *OF* namely 41%, 44.1% and 47.2% and varied Reynolds number 7000, 9000 and 11000. The result show that as the oxygen fraction increase the flame become stronger which result in improved reaction kinetic. This is caused by the associate increase in flame speed according to the measurements of flame speed by Kutne et al. [40]. Moreover, increasing the OF moves the flame toward the burner throat indicating higher flame speed. Figure 18 captured at constant oxygen fraction 42% and different equivalence ratio 0.450, 0.600 and 0.750. The images were captured at different inlet velocity 5.14, 5.19 and 6.21 m/s and different Reynolds number 9000 and 11000. The images show that as the equivalence ratio decrease the flame length become shorter and the flame becomes weak until blow-out occur. This caused by insufficient fuel in the flame zone and lower burning velocity than the flow velocity. This result agreed with the finding of Rashwan et al. [113]. According to these results, oxygen fraction and equivalence ratio have a major effect on flame macrostructure and stability while Reynolds number and velocity have a minor effect.

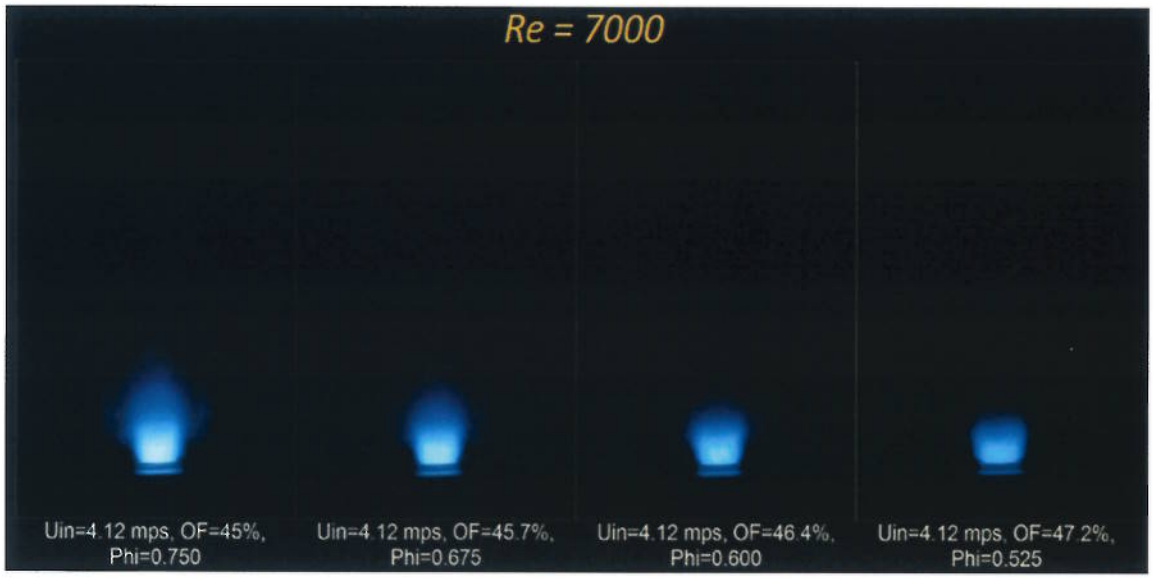

Figure 16 Comparison of flame macrostructure at fixed Reynolds number and inlet velocity 7000, 4.12 m/s over a range of oxygen fraction and equivalence ratio.

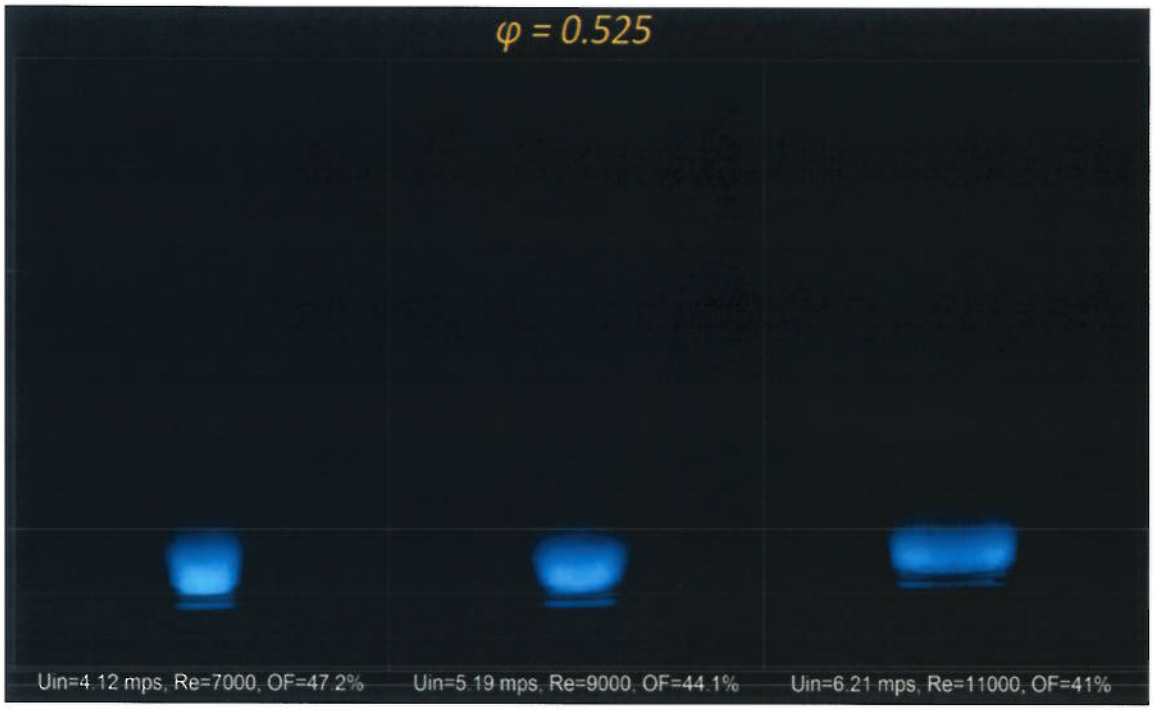

Figure 17 Comparison of flame macrostructure at fixed equivalence ratio 0.525 for different inlet velocities, Reynolds numbers and oxygen fractions.

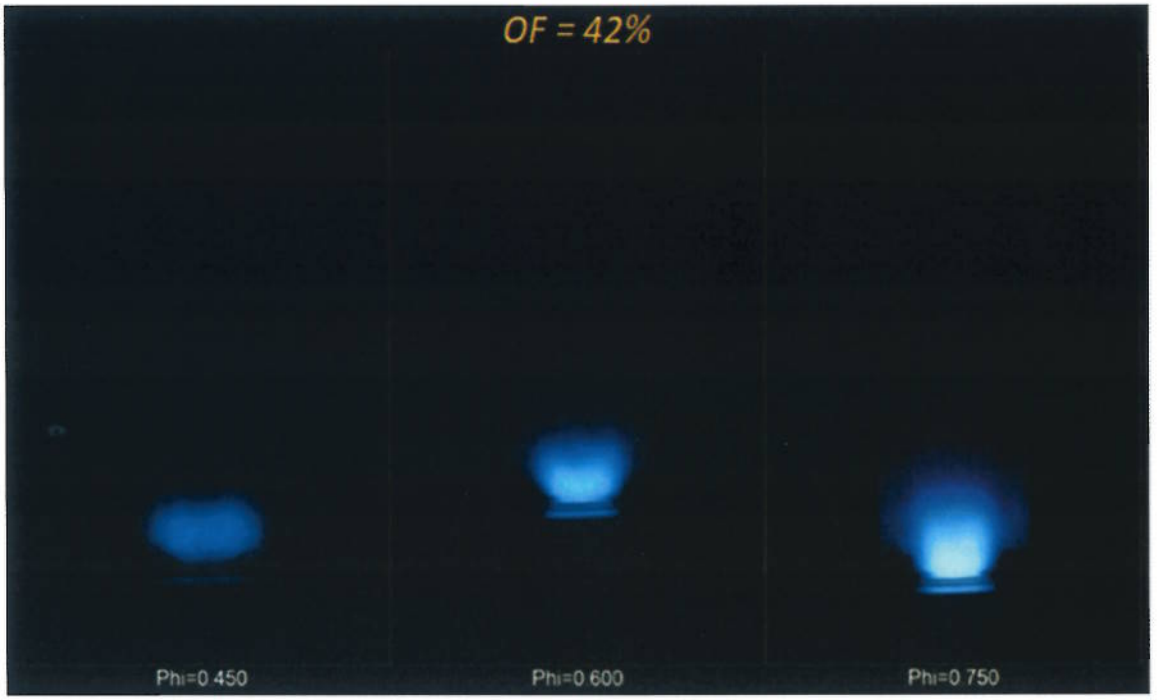

Figure 18 Comparison of flame macrostructure at fixed oxygen fraction 42% for different equivalence ratios.

4.3.5 Analysis of flame macrostructure at fixed T_{ad} through fixed φ and OF over a range of U_{in} and Re

Figure 19 shows the flame images at constant T_{ad} 2100 K. The flames were imaged at constant equivalence ratio 0.6 and constant oxygen fraction 41.2 % with varying the inlet velocity and inlet Reynolds number. The images almost have an identical shape. The results show that keeping T_{ad} constant at 2100 k will give a similar shape for all flames although inlet velocity and Reynolds number are different from one flame to another. This finding agrees with Abdelhafez et al. [128]. They concluded that keeping T_{ad} constant with varying the OF from 50% to 70% and the equivalence ratio from 0.38 to 0.58 will result in having an identical shape for all examined flames. Here we have constant T_{ad} with changing inlet velocity 3.98-6.25 m/s and different Reynolds number 7000, 8000, 9000 and 11000 at constant equivalence ratio and constant oxygen fraction

0.6 and 41.2%. A remarkable conclusion can be made here that despite changing the inlet velocity, oxygen fraction, equivalence ratio and Reynolds number at constant T_{ad}, all flames have an identical shape which means a direct relation between the T_{ad} and the flame shape.

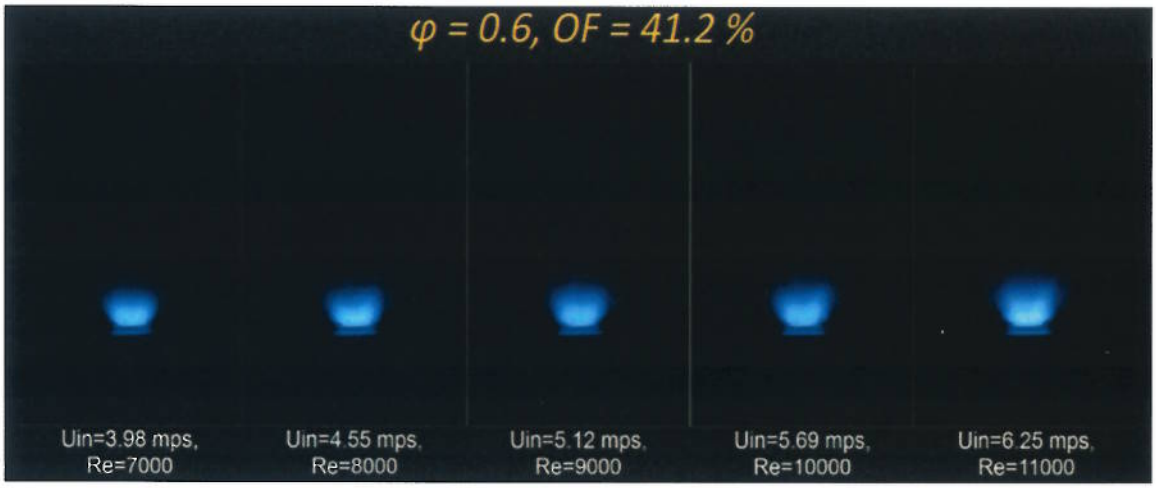

Figure 19 Comparison of flame macrostructure at fixed T_{ad} 2100 K through fixed φ and OF over a range of U_{in} and Re.

4.3.6 Analysis of flame macrostructure at fixed power density over a range of U_{in}, OF, and φ at different inlet Re

The power density was described in equation (3) as follows: -

$$PD = \frac{\dot{m}_{CH4} \times HV_{CH4}}{P \times V_C}$$

Where $\dot{m}_{CH4}$is the mass flow rate of CH_4 calculated based on the operating φ and OF in kg/s, HV_{CH4} is the standard heating value of CH_4 55.5 MJ/kg [133], P is the atmospheric pressure in bar and V_C is the volume of the combustion chamber which is constant. So, the variable element we have here is the mass flow rate of CH_4 which means that power density is directly proportional to fuel flow rate. Figure 20 Show a comparison of flame

macrostructure at fixed power density over a range of inlet velocity, oxygen fraction and equivalence ratio at different inlet *Re*: (top) *Re*=7,000, (middle) *Re*=9,000, and (bottom) *Re*=11,000.

The first row shows flame images at constant Reynolds number over a range of inlet velocity from 3.91 m/s to 4.33 m/s and oxygen fraction from 37.5% to 35.7%. The Reynolds number increases to 9000 in the second row with different inlet velocity and oxygen fraction 4.94-5.45 m/s and 35%-52.3%. In the third row the images were captured at Reynolds number equal to 11000 over a range of inlet velocity and oxygen fraction 5.94-6.51 m/s and 32.5%-48.9%. All the flames were taken at the same equivalence ratio 0.750, 0.675, 0.6, 0.525 and 0.45 for the different Reynolds number. It is noticed that at Re = 7000 the flames have almost an identical shape with minimum OF value equal to 37.5%. When the Reynolds number increase to 9000, all flames have an identical shape similar to first row flame microstructure except the first flame which has a V-shape caused by decreasing the OF to 35%. At Re = 11000, the flame shape is almost identical for all images except the first two images that captured at low oxygen fraction 32.5% and 35.5%, they have a V-shape. Its observed that at constant power density, the flame shape is almost identical for the captured flames even if it's taken at different Reynolds number, inlet velocity and equivalence ratio but, when the OF reduced below 37.5% the flames shape turn to V-shape. It can also be seen that reducing the T_{ad} result in more compact and strong flame.

Figure 20 Comparison of flame macrostructure at fixed power density over a range of inlet velocity, oxygen fraction and equivalence ratio at different inlet *Re*.

4.4 Temperature Analysis

To quantify the effects of *OF* and *Re* on the rates of reaction kinetics within the combustor, local temperature was recorded axially (at different centerline locations above the burner tip) and radially (at different heights, typically h_1=6.35 cm, h_2=7.62 cm and h_3=8.89 cm) at fixed φ of 0.5, as per figures 21 and 22 respectively. While performing temperature measurements, the flame was approached as close as possible to avoid interference of the thermocouple probe with the generated turbulent reacting flow field and to prevent melting of the probe due to the elevated temperature within the flame core. The temperature plots in figures 21 and 22 serve as data base for validating the developed numerical models for handling the turbulent reacting flow under oxy-combustion conditions, in addition to providing quantification of the effects of *OF* and *Re* on flame temperature. Axial and radial temperature profiles, recorded at fixed *Re* of 7,000, show hotter flame at higher *OF*, as per the top plots in figures 21 and 22. Very close to the flame, at axial distance of 6.35 cm, increasing *OF* from 50% to 55% resulted in significant temperature rise of about 200 degrees as per figure 21 (top plot). The flames are of V-shape (see figure 13) and stabilized in the ISL, where temperature is having a maximum value, then, the temperature drops towards the reactor wall, as per figure 22. An inner recirculation zone (IRZ) is created in the center-zone of the combustor keeping the temperature below the maximum flame temperature within the central IRZ, as per figure 22, due to mixing between burned and unburned gases. These results confirm the key role of *OF* in controlling reaction rates within the combustor under oxy-combustion conditions. As per figures 21 and 22 (bottom plots), the results recorded at fixed *OF* 50%

show slightly hotter flames at higher *Re*. At axial distance of 6.35 cm, around 100 degrees increase in temperature is obtained when *Re* increases from 7,000 to 9,000 as shown in figure 21 (bottom plot). This may be attributed to the increase in U_{in}, which results in higher turbulence intensity and improved flame stability.

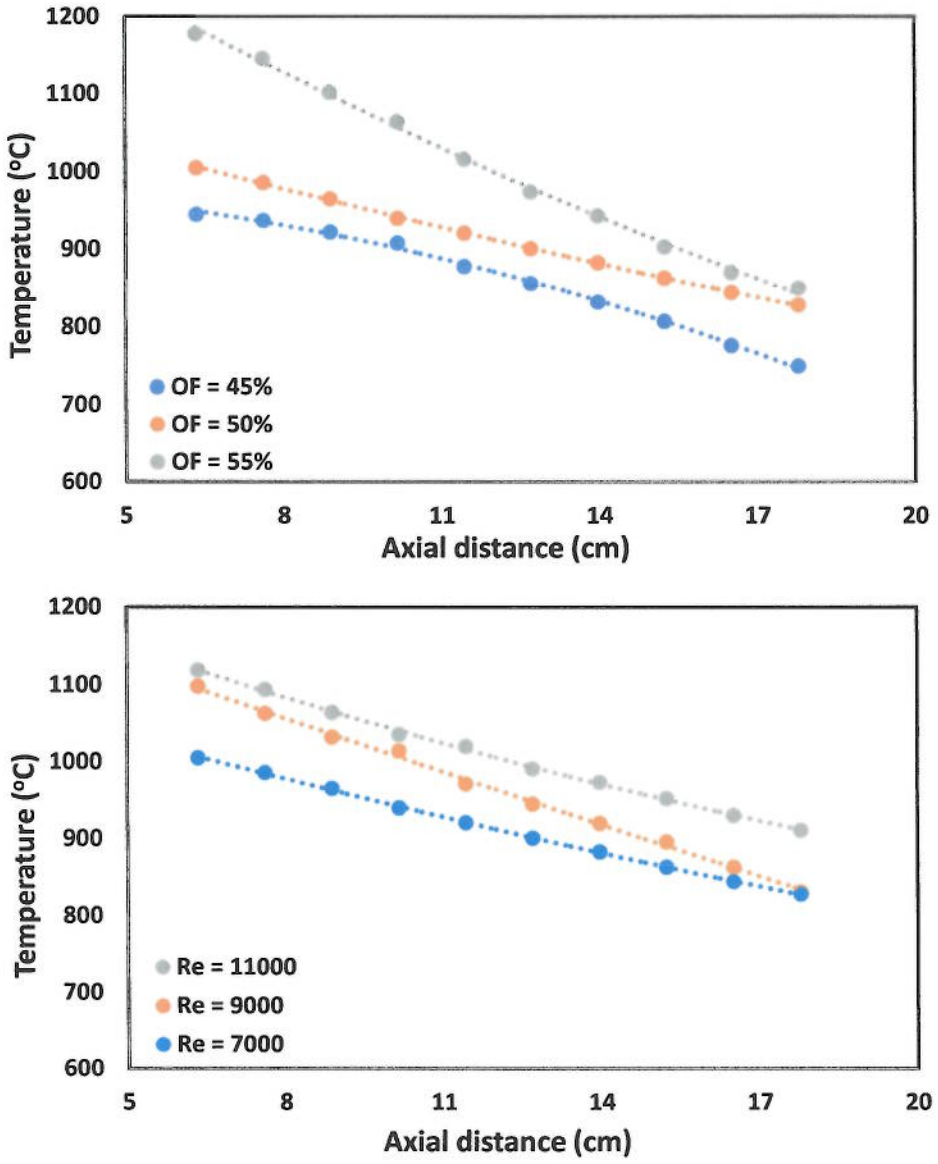

Figure 21 Axial temperature distributions (from the burner tip) at fixed φ of 0.5; (top): effect of *OF* at *Re*=7000 and (bottom): effect of *Re* at *OF*=50%.

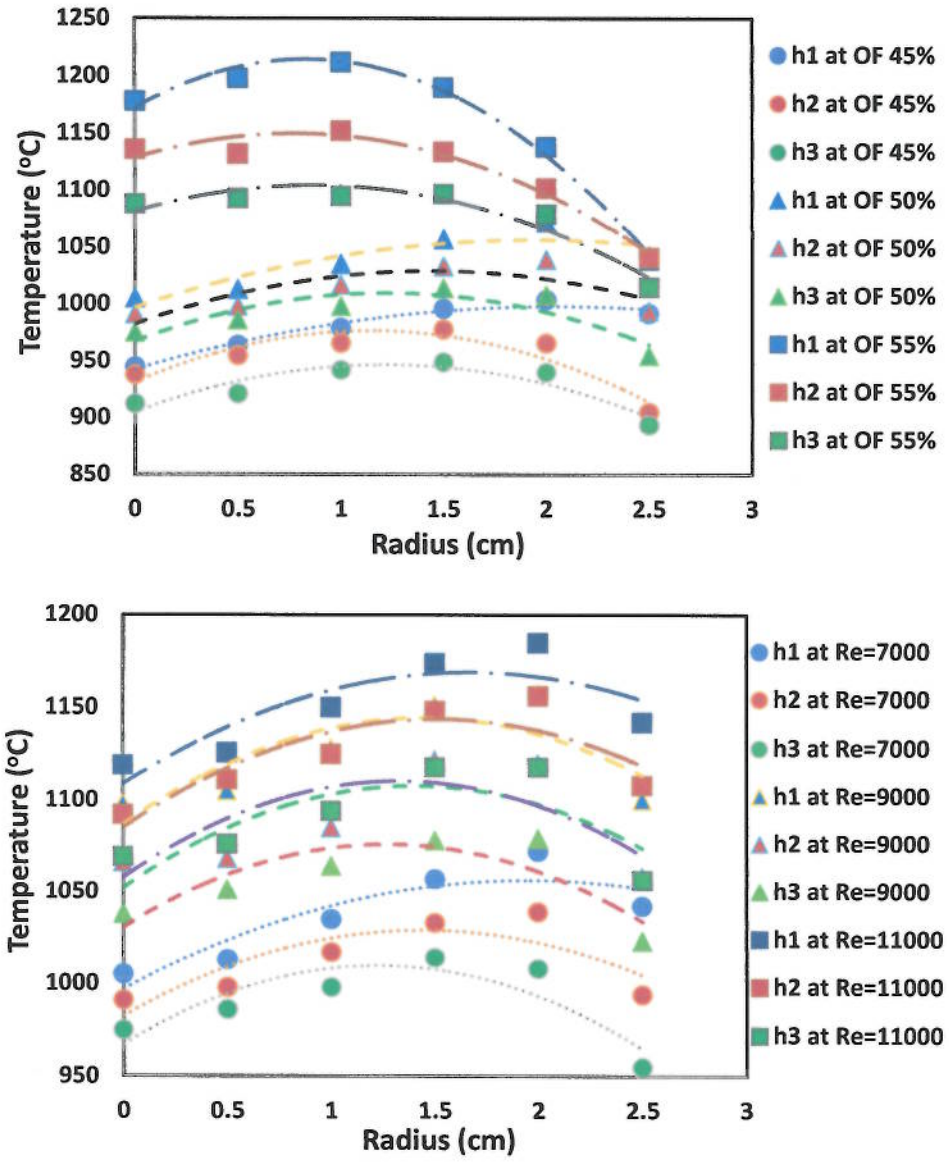

Figure 22 Radial temperature distributions at different heights (h_1=6.35 cm, h_2=7.62 cm and h_3=8.89 cm) and at fixed φ of 0.5; (top): effect of *OF* at *Re*=7000 and (bottom): effect of *Re* at *OF*=50%.

CHAPTER 5

CONCLUSIONS

In this study, the effects of inlet *Re* on static stability limits and changes in macrostructure of premixed oxy-methane flames were examined in a swirl-stabilized gas turbine model combustor. For this purpose, three sets of experiments were performed, each under fixed *Re*, namely 7,000, 9,000 and 11,000. Two-dimensional stability maps, function of φ and *OF*, were generated under fixed *Re* operation, and presented on contour plots of U_{in}, *PD* and T_{ad} to explore their effects on flame static stability limits. The different flame stabilization modes and the changes in flame macrostructure toward the limits were identified based on flame visualization. The effects of φ, *OF*, U_{in}, T_{ad} and *Re* on flame stability were investigated. Temperature measurements are provided to serve as data base for validating the numerical models and to quantify the effects of *OF* and *Re* on flame hotness and stability. Based on this study, the following can be stated:

- The operation of premixed swirl-stabilized oxy-methane flame is not possible for *OF* ranges below 29% and above 70%.
- The flashback limit is mainly controlled by the reaction kinetics rates which control the flame speed at flashback.
- All flames under all operating *Re* values blow-out at the same combustor *PD* indicating its leading role in controlling the lean blow-out stability limit of the oxy-flames.

- Increasing Re shifts the blow-out limit to the leaner side resulting in wider stable flame operability.
- Flame transition from the ISL to the ORZ is observed at certain value of φ controlled mainly by the value of U_{in}.
- Increasing U_{in} delays the flame transition, from the ISL to the ORZ, towards leaner operation and closer to the blow-out limit.
- Holding one flow characteristic parameter (Re) and one flame characteristic parameter (T_{ad}) fixed results in similar flame macrostructures.
- The flames do not hold similar macrostructure neither at flashback nor at blow-out limits.
- Oxygen fraction is a major controlling parameter of stability and macrostructure of the oxy-flames.
- At higher Re operation, the flame encounters successive stabilization in the ORZ, lift-off and blow-out stabilization modes.
- At lower Re, the flames stabilized in the ORZ then it directly blow-out without being lifted.

References

1. M.V. Hoeven, "CO2 emission from fuel combustion," Paris, France, IEA, p. 12-27, 2011.
2. J. Hansen, M. Sato, R. Ruedy, K. Lo, D.W. Lea, and M. Elizade, "Global temperature change," Proc Natl Acad Sci, 103(39), pp. 14288-93, 2006.
3. W. Fiveland, "An overview to Alstom's R&D activities on oxy-combustion technology application for power generation industry," In Proc 2nd workshop of IEA GHG, Windsor, USA, Int Oxy-Comb Network, 2007.
4. L. Zheng, "Oxy-fuel combustion for power generation and carbon dioxide (CO2) capture," Cambridge, UK, Woodhead Publishing Limited, p.3, 2011.
5. E.H. Chui, A.J. Majeski, M.A. Douglas, Y. Tan, and K.V. Thambimuthu, "Numerical investigation of oxy-coal combustion to evaluate burner and combustor design concepts," Energy, 29, pp. 1285-96, 2004.
6. P. Buhre, L.K. Elliott, C.D. Sheng, R.P. Gupta, and T.F. Wall, "Oxy-fuel combustion technology for coal-fired power generation," Prog Energy Combust Sci, 31, pp. 283-307,2005.
7. M. B. Toftegaard, J. Brix, P.A. Jensen, P. Glarborg, and A.D. Jensen, "Oxy-fuel combustion of solid fuels," Prog Energy Combust Sci, 36, pp. 581-625, 2010.
8. G. Scheffknecht, L. Al-Makhadmeh, U. Schnell, and J. Maier, "Oxy-fuel coal combustion-A review of the current state-of-the-art," Int J Greenh Gas Control, 5, pp. 16-35, 2011.
9. J. Oh, and D. Noh, "Laminar burning velocity of oxy-methane flames in atmospheric condition," Energy, 45, pp. 669-75, 2012.

10. A. F. Ghoniem, "Needs, resources and climate change: clean and efficient conversion technologies," Prog Energy Combust Sci, 37 pp. 15-51, 2011.

11. J. Riaza, L. Alvarez, M.V. Gil, C. Pevida, J.J. Pis, and F. Rubiera, "Effect of oxy-fuel combustion with steam addition on coal ignition and burnout in an entrained flow reactor," Energy, 36, pp. 5314-9, 2011.

12. J. Warnatz, U. Mass, and R.W. Dibble, "Combustion," Springer, New York, chap. 17, 1996.

13. "https://www.globalccsinstitute.com/understanding-ccs/how-ccs-works-capture."

14. "https://www.worlddata.info/asia/saudi-arabia/energy-consumption.php."

15. L. Chen, S.Z. Yong, and A.F. Ghoniem,"Oxy-fuel Combustion of Pulverized Coal: Characterization, Fundamentals, Stabilization and CFD Modeling," Process in Energy and Combustion Science, 38, pp. 156–214, 2012.

16. P. Glarborg, and L.L. Bentzen, "Chemical effect of a high CO_2 concentration in oxy-fuel combustion of methane," Energy Fuels, 22, pp. 291–296, 2007.

17. A. Amato, B. Hudak, and P. D'Carlo, "Methane Oxy-combustion for low CO_2 cycle: blow-off measurments and analysis," Journal of Engineering for Gas Turbines Power 133, pp. 61-503, 2011.

18. A.P. Shroll, S.J. Shanbhogue, and A.F. Ghoniem, "Dynamic stability characterstics of premixed methane oxy-combustion" Journalof Engineering for Gas Turbines Power,134, 2012.

19. H. Watanabe, S.J. Shanbhogue, and A.F. Ghoniem, " Impact of equivalence ratio on the macrostructure of premixed swirling CH4/air and CH_4/O2/CO2 flames," ASME Turbo Expo (GT2015-43224), 2015.

20. D. Bongartz, and A.F. Ghoniem, "Chemical kinetics mechanism for oxy-fuel combustion of mixtures of hydrogen sulfide and methane," Combust. Flame, 162, pp. 544–553, 2015.

21. P. Jourdaine, C. Mirat, J. Beaunier, Y. Joumani, and T. Schuller, "Effect of Quarl on the Stabilization of N2- and CO2-diluted swirling oxy-flames," inProceedings of the European Combustion Meeting, 2015.

22. P. Kutne, B.K. Kapadia, W. Meier, and M. Aigner, "Experimental analysis of the combustion behaviour of oxy-fuel flames in a gas turbine modelcombustor," Proc. Combust. Inst., 33, pp. 3383–3390, 2011.

23. "http://web.mit.edu/16.unified/www/FALL/thermodynamics/notes/node111.html."

24. Manuscript submitted to Elsevier as part of the Combustion Treatise Series formerly published by Academic Press.

25. "http://cornerstonemag.net/overview-of-oxy-fuel-combustion-technology-for-co2-capture/."

26. S. Kim, K. Arghode, and K. Gupta, "Flame characteristics of hydrogen-enriched methane–air premixed swirling flames," International Journal of Hydrogen Energy, 34, pp. 1063-1073, 2009.

27. R. Seiser, L. Trutte, and K. Seshadri, "Extinction of partially premixed flames," Proc Combust Inst, 29, pp. 1551–7, 2002.

28. Y.L. Chan, M.M. Zhu, Z.Z. Zhang, P.F. Liu, and D.K. Zhang, "The effect of CO2 dilution on the laminar burning velocity of premixed methane/air flames," In The 7th international conference on applied energy, 75 pp. 3048–53, 2015.

29. Y.H. Li, G.Y. Chen, Y.C. Lin, and Y.C. Chao, "Effects of flue gas recirculation on the premixed oxy-methane flames in atmospheric condition," Energy, 89, pp. 845-857, 2015.

30. H. Watanabe, S. J. Shanbhogue, and A. F. Ghoniem, in Proceedings of ASME Turbo Expo (GT2015-43224), 2015.

31. P. Griebel, E. Boschek, and P. Jansohn, "Lean Blowout Limits and NOx Emissions of Turbulent, Lean Premixed, Hydrogen- Enriched Methane/Air Flames at High Pressure," Combustion Research.

32. M. Jamal, H. Ibrahim, M. Ali, M. Elmahallawy, A. Abdelhafez, A. Nemitallah, S. Rashwan, and A. Habib, "Structure and Lean Extinction of Premixed Flames Stabilized on Conductive Perforated Plates", Energy and Fuels.

33. D. Fritsche, M. Furi, and K. Boulouchos, "An Experimental Investigation of Thermoacoustic Instabilities in a Premixed Swirl-Stabilized Flame", Combustion and Flame, 151, pp. 29–36, 2007.

34. D.W. Davis, P.L. Therkelsen, D. Littlejohn, and R.K. Cheng, "Effect of Hydrogen on the Thermo-Acoustics Coupling Mechanisms of Low-Swirl Injector flames in a Model Gas Turbine Combustor," Proceedings of the Combustion Institute, 34, pp. 3135–3143, 2013.

35. K. Kashinath, and M.P. Juniper, "Nonlinear Phenomena in Thermo acoustics: Comparison between Single-Mode and Multi-Mode Methods," 19th International Congress on Sound and Vibration, Vilnius, Lithuania, July 8-12, 2012.

36. P. L. Therkelsen, J. Portillo, D. Littlejohn, S.M. Martin, and R.K. Cheng, "Self-induced Unstable Behaviors of CH4 and H2/ CH4 Flames in a Model Combustor with a Low-Swirl Injector," Combustion and Flame, 160, pp. 307–321, 2013.

37. K. Lee, H. Kim, P. Park, S. Yang, and Y. Ko, "CO2 radiation heat loss effects on NOx emissions and combustion instabilities in lean premixed flames," Fuel, 106, pp. 682-9, 2013

38. NP. Yadav, and A. Kushari, "Visualization of recirculation in low aspect ratio dumpCombustor," J Flow Vis Image Process, 16, pp. 127-36, 2009.

39. RL. Speth, and AF. Ghoniem, "Using a strained flame model to collapse dynamic mode data in a swirl-stabilized syngas combustor," Proc Combust Inst, 32, pp. 2993-3000, 2009.

40. P. Kutne, B.K. Kapadia, W. Meier, and M. Aigner, "Experimental analysis of the combustion behaviour of oxyfuel flames in a gas turbine model combustor," Proc Combust Inst, 33, pp. 3383-90, 2011.

41. S.S. Rashwan, A.H. Ibrahim, T.W. Abou-Arab, M.A. Nemitallah, and M.A. Habib, "Experimental investigation of partially premixed methane-air and methane-oxygen flames stabilized over a perforated-plate burner," Appl Energy, 169, pp. 126-137, 2016.

42. S.S. Rashwan, A.H. Ibrahim, T.W. Abou-Arab, M.A. Nemitallah, and M.A. Habib, "Experimental study of atmospheric partially premixed oxy-combustion flames anchored over a perforated plate burner," Energy, 122, pp. 159-167, 2017.

43. K. Kimura, K. Omata, T. Kiga, S. Takano, and S. Shikisima, "Characteristics of pulverized coal combustion in O2/CO2 mixtures for CO2 recovery,"Energy Convers. Manage, 36, pp. 805-8, 1995.

44. T. Fujimori, and T. Yamada, "Realization of oxyfuel combustion for near zero emission power generation," Proceedings of the Combustion Institute, 34, pp. 2111–2130, 2013.

45. Q. Zhang, D.R. Noble, and T. Lieuwen, "Blowout Measurements in a Syngas-Fired Gas Turbine Combustor," The 22nd Annual International Pittsburgh Coal Conference, Pittsburgh, PA.September pp. 12-15, 2005.

46. Z. Riahi, H. Bounaouara, I. Hraiech, M. Mergheni, J. Sautet, and S. Nasrallah, "Combustion with mixed enrichment of oxygen and hydrogen in lean regime," Int J Hydrogen Energy 2016.

47. M.A. Nemitallah, and M.A. Habib, "Experimental and numerical investigations of an atmospheric diffusion oxy-combustion flame in a gas turbine model combustor," Applied Energy, 111, pp. 301–415, 2014.

48. T. Garcıa, and J. Ballester, "Operational Issues in Premixed Combustion of Hydrogen-Enriched and Syngas Fuels," International Journal of Hydrogen Energy, 40, pp. 1229-1243, 2015.

49. J.D. Thornton, B.T. Chorpening, T.G. Sidwell, P.A. Strakey, E.D. Huckaby, and K.J. Benson, "Flashback Detection Sensor for Hydrogen Augmented Natural Gas Combustion," In Proceedings of GT2007-ASME Turbo Expo 2007: Power for Land, Sea, and Air; Montreal, Canada, Paper No. GT2007-27865, pp. 739-746, 2007.

50. S. Daniele, P. Jansohn, and K. Boulouchos, "Experimental Investigation of Lean Premixed Syngas Combustion at Gas Turbine Relevant Conditions: Lean Blow out Limits, Emissions and Turbulent Flame Speed," Combustion colloquie, 2009.

51. D. E. Cavaliere, J. Kariuki, and E. Mastorakos, "A comparison of the blow-off behaviour of swirl-stabilized premixed, non-premixed and spray flames," Flow Turbulant Combustion, 91, pp. 347-372.

52. A. Amato, B. Hudak , and P. D'Carlo, "Measurements and analysis of CO and O2 emissions in CH4/ CO2/ O2 flames," 33, pp. 3399–3405, 2011.

53. S. Hoffmann, P. Habisreuther, and B. Lenze, "Development and assessment of correlations for predicting stability limits of swirling flames," Chem. Eng. Process, 33, pp. 393-400, 2005.

54. F.A. Williams, "Combustion Theory, second ed", The Benjamin/Cummings Publishing Company Inc., California, 1985.

55. N. Peters, and F.A. Williams, "Premixed combustion in a vortex," the Combustion Institute, 22, pp. 495–503, 1989.

56. K. Seshadri, and N. Peters, "The inner structure of methane-air flames," Combustion and Flame, 81, pp. 96–118, 1990.

57. A. Abdulsada, "Flashback and Blow-off Characteristics of Gas Turbine Swirl Combustor", (Ph. D. thesis). Institute of Energy, Cardiff School of Engineering, Cardiff University, pp. 1-188.

58. G. Krieger, A. Campos, M. Takehara, F. da Cunha, and C.A. Veras, "Numerical simulation of oxy-fuel combustion for gas turbine applications," Applied Thermal Engineering, 78, pp. 471-481, 2015

59. Y. Xuan, and G. Blanquart, "Two-dimensional flow effects on soot formation in laminar premixed flames,"Combustion and Flame, 166, pp. 113–124, 2016.

60. S. Seepana, and S. Jayanti, "Flame structure investigations of oxy-fuel combustion," Fuel, 93, pp. 52–58, 2012.

61. R.W. Schefer, D.M. Wicksall, and A.K. Agrawal, "Combustion of Hydrogen-Enriched Methane in a Lean Premixed Swirl-Stabilized Burner," Proc. of the Combustion Institute, Pittsburgh, 29, pp. 843–851.

62. R. Hawkes, and H. Chen, "Direct numerical simulation of hydrogen-enriched lean premixed methane–air flames," Combustion and Flame, 138, pp. 242–258, 2004.

63. H. Erjiang, H. Zuohua, H. Jiajia, and M. Haiyan, "Experimental and numerical study on lean premixed methane–hydrogen–air flames at elevated pressures and temperatures," International Journal of hydrogen energy, 34, pp. 6951 – 690, 2009.

64. M. De La Torre, N. Love, and A. Choudhuri, "Effect of Diluents, Firing Input, and Hydrogen Content on Premixed Oxy-Syngas Flames," 11th International Energy Conversion Engineering Conference,, San Jose, CA., July 14 - 17, 2013.

65. Y. Li, G.B. Chen, and Y.C. Chao, "Effects of flue gas addition on the premixed oxy methane flames in atmospheric condition," Energy Proc, 75, pp. 3054–9, 2015.

66. E.V. Jithin, V.R. Kishore, and R.J. Varghese, "Three-dimensional simulations of steady perforated-plate stabilized propane-air premixed flames," Energy Fuels, 28, pp. 5415-25, 2014.

67. S. Aladawy, J. Lee, and B. Abdelnabi, "Effect of turbulence on NOx emission in a lean perfectly-premixed combustor," Fuel, 208, pp. 160-167, 2017.

68. E. Rathakrishnan, "fundamental of engineering thermodynamics, second edition," department of aerospace engineering, indian institute of technology kanpur.

69. E. Bancalari, P. Chan, and I. Diakunchak, "Advanced hydrogen gas turbine development program," ASME Turbo Expo Power Land Sea, GT2007-27869, 2007.

70. K. Gupta, A. Rehman, and R. Sarviya, "Bio-fuels for the gas turbine: a review," Renew Sustain Energy Rev, 14, pp. 2946-55, 2010.

71. M.K. Elhossaini, "Review of the new combustion technologies in modern gas turbines," progress in gas turbine performance, pp. 953-78, 2013

72. P. Buhre, L.K. Elliott, C.D. Sheng, R.P. Gupta, and T.F. Wall, "Oxy-fuel combustion technology for coal-fired power generation," Prog Energy Combust Sci, 31, pp. 283–307, 2005.

73. M. Kumagami, Y. Ogami, Y. Tamaki, and H. Kobayashi, "Numerical analysis of extremely-rich CH4/O2/H2O premixed flames at high pressure and high temperature considering production of higher hydrocarbons," J Therm Sci Technol, 5, pp. 109–23, 2010.

74. M. Ditaranto, and J. Hals, "Combustion instabilities in sudden expansion oxy-fuel flames," Combust Flame, 146, pp. 493-512, 2006.

75. F. Liu, and O.L. Gulder, "Effects of H2 and H preferential diffusion and unity Lewis number on super adiabatic flame temperatures in rich premixed methane flames," Comb Flame, 143, pp. 264–81, 2005.

76. B. Stelzner, C. Weis, P. Habisreuther, N. Zarzalis, and D. Trimis, "Super-adiabatic flame temperatures in premixed methane flames: A comparison between oxy-fuel and conventional air combustion," Fuel 2017.

77. W. Fick, A. Griffiths, and T. Doherty, "Visualization of the processing vortex core inan unconfined swirling flow," Opt Diagnostics Eng, 2(1), pp. 19–31, 1997.

78. J. Fritz, M. Kroner, and T. Sattelmayer, "Flashback in a Swirl Burner with cylindrical premixing zone," ASME J Eng Gas Turbines Power, 126, pp. 276–83, 2004.

79. M. Kroner, J. Fritz, and T. Sattelmayer, "Flashback limits for combustion induced vortex breakdown in a Swirl Burner," ASME J Eng Gas Turbines Power, 125, pp. 693–700, 2003.

80. F. Kiesewetter, C. Kirsch, J. Fritz, M. Kroner, and T. Sattelmayer, "Two-dimensional flashback simulation in strongly swirling flows," In Proceedings of ASME Turbo Expo, June 16–19, 2003.

81. Y. Sommerer, D. Galley, T. Poinsot, S. Ducruix, F. Lacas, and D. Veynante, "Large eddy simulation in a lean partially premixed swirled burner," J Turbulence, pp. 37–37(1), 2004.

82. X. Wu, "Asymptotic approach to combustion instability," Philos Trans Roy Soc, 363, pp. 1247–59, 2005.

83. J.P. Hathout, M. Fleifil, A.M. Annaswamy, and A.F. Ghoniem, "Active control using fuel injection of time-delay induced combustion instability," AIAA J Propulsion Power, 18(2), pp. 390–9, 2000.

84. J. Fritz, M. Kroner, and T. Sattelmayer, "Flashback in a Swirl Burner with cylindrical premixing zone," ASME J Eng Gas Turbines Power, 126, pp. 276–83, 2004.

85. T. Sattelmayer, M. Kroner, and J. Fritz, "Flashback limits for combustion induced vortex breakdown in a Swirl Burner," ASME J Eng Gas Turbines Power, 125, pp. 693–700, 2003.

86. S. Leibovich, "The structure of vortex breakdown," Annu Rev Fluid Mech, 10, pp. 221–46, 1978.

87. A. Schonborn, P. Sayad, and J. Klingmann, "Influence of precessing vortex core on flame flashback in swirling hydrogen flames," Int. J. Hydrogen Energy 39, pp. 20233-20241.

88. D. Durox, J.P. Moeck, J.F. Bourgouin, P. Morenton, M. Viallon, T. Schuller, and S. Candel, "Flame dynamics of a variable swirl number system and instability control," Combust. Flame, 160, 1729-1742.

89. M.E. Harris, J. Grumer, G. Von Elbe, and B. Lewis, "Burning velocities, quenching, and stability data on nonturbulent flames of methane and propane with oxygen and nitrogen," In Third Symposium on Combustion, Flame and Explosion Phenomena, pp. 80-89.

90. C. Zhiguang, Q. Chaokui, and Z. Yangjun, "Flame stability of partially premixed combustion for PNG/LNG interchangeability," J. Nat. Gas. Sci. Eng., 21, pp. 467-473.

91. N. Shelil, "Flashback Studies with Premixed Swirl Combustion (Ph.D. thesis)," Institute of Energy, Cardiff University, pp. 1-227.

92. D. Beerer, V. McDonell, P. Therkelsen, and R.K. Cheng, "Flashback and turbulent flame speed measurements in hydrogen/methane flames stabilized by a lowswirl injector at elevated pressures and temperatures," ASME J. Eng. Gas. Turbines Power, 136, 031502-1-9.

93. B. Shi, J. Hu, and S. Ishizuka, "Carbon dioxide diluted methane/oxygen combustion in a rapidly mixed tubular flame burner," Combust Flame, pp. 420-30, 2015.

94. X. Hu, Q. Yu, J. Liu, and N. Sun, "Investigation of laminar flame speeds of CH4/O2/CO2 mixtures at ordinary pressure and kinetic simulation," Energy, 70, pp. 626-634, 2014.

95. T. Williams, C. Shaddix, and R. Schefer, "Effect of syngas composition and CO2-diluted oxygen on performance of a premixed swirl-stabilized combustor,"Combust Sci Technol, 180, pp. 64-88, 2007.

96. K. Andersson, and F. Johnsson, "Flame and radiation characteristics of gas-fired O2/CO2 combustion," 86, pp. 656–68, 2007.

97. P. Heil, D.Torporov, H. Stadler, S. Tschunko, M. Forster, and R. Kneer, "Development of an oxy-coal swirl burner operating at low O2 concentrations," 88, pp. 1269–74, 2009.

98. M. Aliyu, M. Nemitallah, S. Said, and M. Habib, "Characteristics of H2-enriched CH4/O2 diffusion flames in a swirl-stabilized gas turbine combustor," international journal of hydrogen energy, pp. 1-15, 2015.

99. B. Yu, S. Kum, C. Lee, and S. Lee, "Study on the combustion characteristics of a premixed combustion system with exhaust gas recirculation," 61, pp. 345–353, 2013.

100. M. Habib, M. Nemitallah, P. Ahmed, M. Sharqawy, H. Badr, I. Muhammad, and M. Yaqub, "Experimental analysis of oxygen-methane combustion inside a gas turbine reactor under various operating conditions," Energy, pp. 1-10, 2015.

101. S. Seo, "Parametric study of lean-premixed combustion instability in a pressurized model gas turbine combustor (Ph.D. thesis)," University Park, PA: Department of Mechanical and Nuclear Engineering, The Pennsylvania State University, 1999.

102. "https://www.nuclear-power.net/nuclear-engineering/fluid-dynamics/reynolds-number/."

103. N. Guilbert, A. Mura, B. Boust, and M. Champion, "Study of premixed combustion instabilities using phase locked tomography PIV," 14th Int Symp on Applications of Laser Techniques to Fluid Mechanics, Lisbon, Portugal, 07-10 July, 2008.

104. H. Carlsson, E. Nordstrom, A. Bohlin, Y. Wu, B. Zhou, Z. Li, M. Alden, P. Bengtsson, and X. Bai, "Numerical and experimental study of flame propagation and quenching of lean premixed turbulent low swirl flames at different Reynolds numbers," Combustion and Flame, 162, pp. 2582–2591, 2015.

105. M. Baigmohammadi, S.Tabejamaat, and Y. Farsiani, "Experimental study of the effects of geometrical parameters, Reynolds number, and equivalence ratio on methane–oxygen premixed flame dynamics in non-adiabatic cylindrical meso-scale reactors with the backward facing step,"Chemical Engineering Science, 132, pp. 215-233, 2015.

106. C. Liu, S. Shy, M. Peng, C. Chiu, and Y. Dong, "High-pressure burning velocities measurements for centrally-ignited premixed methane/air flames interacting with

intense near-isotropic turbulence at constant Reynolds numbers,"Combustion and Flame, 159, pp. 2608–2619, 2012.

107. C. Chiu, Y. Dong, and S. Shy, "High-pressure hydrogen/carbon monoxide syngas turbulent burning velocities measured at constant turbulent Reynolds numbers," International Journal of Hydrogen Energy, 37, pp. 10935-10946, 2012.
108. P. Gobbato, M. Masi, A. Cappelletti, and M. Antonello, "Effect of the Reynolds number and the basic design parameters on the isothermal flow field of low-swirl combustors," Experimental Thermal and Fluid Science, 84, pp. 242–250, 2017
109. P.A. Dellenback, D.E. Metzger, and G.P. Neitzel, "Measurement in turbulent swirling flow through an abrupt axisymmetric expansion," AIAA J., 26, pp. 669–681, 1988.
110. N. Syred, and J.M. Beer, "Combustion in swirling flows," a review, Combust. Flame, 23, 1974.
111. H. Watanabe, S.J. Shanbhogue, and A.F. Ghoniem, " Impact of equivalence ratio on the macrostructure of premixed swirling CH4/air and CH_4/O2/CO2 flames," ASME Turbo Expo (GT2015-43224), 2015.
112. P. Jourdaine, C. Mirat, J. Caudal, A. Lo, and T. Schuller, "A compression between the stabalization of premixed swirling CO_2-diluted methane Oxy-flames and methane air/flames," Fuel, 201, pp. 156-164, 2017.
113. S.S. Rashwan, A. H. Ibrahim, T.W. Abou-Arab, M. A. Nemitallah, and M. A. Habib, "Experimental investigation of partially premixed methane–air and methane–oxygen flames stabilized over a perforated-plate burner," Applied Energy, 169, pp. 126–137, 2016.

114. R.M. Fearn, T. Mullin, and K.A. Cliffe, "Nonlinear flow phenomena in a symmetric sudden expansion," Journal Fluid of Mechanics, 211, pp. 595–608, 1990.

115. S.H. Lo, P.R. Voke, and N.J. Rockliff, "Three dimensional vortices of a spatially developing plane jet," International Journal of Fluid Dynamic, 4, 2000.

116. S. Ducruix, T. Schuller, D. Durox, and S. Candel, "Combustion dynamics and instabilities: Elementary coupling and driving mechanisms," Journal of Propulsion and Power, 19, pp. 722–734, 2003.

117. A. Soika, F. Dinkelacker, and A. Leipertz, "Measurement of the resolved flame structure of turbulent premixed flames with constant Reynolds number and varied stoichiometry," The Combustion Institute, pp. 785–792, 1998.

118. F. Richecoeur, and C. Kyritsis, "Experimental study of flame stabilization in low Reynolds and Dean number flows in curved mesoscale ducts," Proceedings of the Combustion Institute, 30, pp. 2419–2427, 2005.

119. M. Bollinger, and T. Williams. "Effect of Reynolds number in the turbulent-flow range on flame speeds of bunsen-burner flames," Flight Propulsion Research Laboratory Cleveland, Ohio.

120. W.E. Kaskan, "The dependence of flame temperature on mass burning velocity," Symposium (Intl.) on Combustion, 6, pp. 134-143, 1957.

121. A. Van Maaren, D.S. Thung, and L.P. de Goey, "Measurement of Flame Temperature and Adiabatic Burning Velocity of Methane-Air Mixtures," Combustion Science and Technology, 96, pp. 327-344, 1994.

122. A.N. Mazas, B. Fiorina, D.A. Lacoste, and T. Schuller, "Effects of water vapor addition on the laminar burning velocity of oxygen-enriched methane flames," Combustion and Flame, 158, pp. 2428-2440, 2011.

123. A. Chaparro, and M. Cetegen, "Blowoff characteristics of bluff-body stabilized conical premixed flames under upstream velocity modulation," Mechanical Engineering Department, University of Connecticut,Combustion and Flame, 144, pp. 318–335, 2006.

124. J. Yoon, M. Kim, J. Hwang, J. Lee, and Y. Yoon, "Effect of fuel-air mixture velocity on combustion instability of a model gas turbine combustor," Applied Thermal Engineering, 54, pp. 92-101, 2013.

125. N. Papanikolaou, and I. Wierzba, "The effect of Co-flowing stream velocities on the flow characterstics of jets issuing from elliptic nozzels," Journal of Energy Resources Technol, 118, pp. 134–139, 1996.

126. W. Kaskan, "The dependence of flame temperature on mass burning velocity," Symposium (Intl.) on Combustion, 6, pp. 134-143, 1957.

127. A. Maaren, D. Thung, and L. de Goey, "Measurement of Flame Temperature and Adiabatic Burning Velocity of Methane-Air Mixtures," Combustion Science and Technology, 96, pp. 327-344, 1994.

128. A. Abdelhafez, S.S. Rashwan, M. A. Nemitallah, and M. A. Habib, "Stability map and shape of premixed CH4/O2/CO2 flames in a model gas turbine combustor," Applied Energy, 215, pp. 63-74, 2018.

129. A.N. Mazas, B. Fiorina, D.A. Lacoste, and T. Schuller, "Effects of water vapor addition on the laminar burning velocity of oxygen-enriched methane flames," Combustion and Flame, 158, pp. 2428-2440, 2011.

130. F. Coppens, J. De Ruyck, and A. Konnov, "The effects of composition on burning velocity and nitric oxide formation in laminar premixed flames of CH4+H2+O2+N2," Combustion and Flame, 149, pp. 409-417, 2007.

131. C. Prathap, A. Ray, and M. Ravi, "Investigation of nitrogen dilution effects on the laminar burning velocity and flame stability of syngas fuel at atmospheric condition," Combustion and Flame, 155, pp. 145-160, 2008.

132. S. Taamallah, NW. Chakroun, H. Watanabe, SJ. Shanbhogue, and AF. Ghoniem, "On the characteristic flow and flame times for scaling oxy and air flame stabilization modes in premixed swirl combustion," Proc. Combust. Inst., 36, pp. 3799–807, 2015.

133. Y.A. Cengel, and M.A. Boles " Thermodynamics: an engineering approach," 8th edition, 2015.

Vitae

Name	Shabeeb Ali Alkhaldi	
Nationality	Saudi	
Date of Birth	17/12/1991	
Email	Shabeeb.1122@hotmail.com	
Address	2811-Alkheel Street	
	Eastern province, Saudi Arabia.	
Academic Background	Master of Science (M.S.)	April, 2018
	Mechanical Engineering Department	
	King Fahad University of Petrolum & Minerals	
	Dhahran, Saudi Arabia.	
	Bachelor of Science (B.S)	May, 2014
	Mechanical Engineering Department	
	Jubail University College	
	Jubail Industrial City, Saudi Arabia.	

Papers

1. Nemitallah MA, Alkhaldi S, Abdelhafez A, Habib MA. On the effect of Reynolds number on the macrostructure and static-stability limits of oxy-methane flames in a premixed swirl combustor. Submitted to Energy (EGY-D-18-02400).